

Manuscript version: Author's Accepted Manuscript

The version presented in WRAP is the author's accepted manuscript and may differ from the published version or Version of Record.

Persistent WRAP URL:

<http://wrap.warwick.ac.uk/140718>

How to cite:

Please refer to published version for the most recent bibliographic citation information. If a published version is known of, the repository item page linked to above, will contain details on accessing it.

Copyright and reuse:

The Warwick Research Archive Portal (WRAP) makes this work by researchers of the University of Warwick available open access under the following conditions.

© 2020 Elsevier. Licensed under the Creative Commons Attribution-NonCommercial-NoDerivatives 4.0 International <http://creativecommons.org/licenses/by-nc-nd/4.0/>.



Publisher's statement:

Please refer to the repository item page, publisher's statement section, for further information.

For more information, please contact the WRAP Team at: wrap@warwick.ac.uk.

1 **Devolatilisation Characteristics of Coal and Biomass with Respect to**
2 **Temperature and Heating Rate for Hlsarna Alternative Ironmaking**
3 **Process**

4 **Darbaz Khasraw^{a,*}, Stephen Spooner^a, Hans Hage^b, Koen Meijer^b, Zushu Li^a**

5 ^aWMG, University of Warwick, Coventry, UK

6 ^bTata Steel IJmuiden, The Netherlands

7

8 **HIGHLIGHTS**

- 9 • **Devolatilisation behaviours of different carbon sources investigated for Hlsarna alternative**
10 **ironmaking process.**
- 11 • **Maximum peaks of evolved gases from VTF-QMS corresponded well to DTG curves.**
- 12 • **The kinetic parameters for coal and biomass samples were determined.**
- 13 • **Biomass pre-treatment temperature suggested to produce chars with similar properties to coal**
14 **injected in Hlsarna.**

15 **Abstract:** Hlsarna process offers a novel low CO₂ emission alternative to the blast furnace for
16 primary iron production. This new smelting ironmaking technology is flexible in raw material usage
17 such as the substitution of biomass for coal as a reductant. Reduction is conducted through multiple
18 mechanisms within the smelting vessel including gaseous reaction products from thermal
19 decomposition of volatile matters reacting directly with iron oxide containing slags and injected iron
20 ore. In this study, four coals with notable differences in volatile matter content along with two
21 biomass samples sourced from wood and grass origins were investigated for the selection of suitable
22 fuel mix. Thermogravimetric analysis (TGA) was used to measure the weight loss of the

23 carbonaceous materials and a vertical tube furnace coupled with a quadrupole mass spectrometer
24 (VTF-QMS) was employed for off-gas analysis during the devolatilisation. During TGA tests the
25 samples were heated under a 99.9999 % argon atmosphere to 1500 °C at three different heating
26 rates to investigate the kinetics of thermal decomposition for these materials. Through use of the
27 Kissinger– Akahira–Sonuse model an average activation energy was determined as a function of the
28 conversion degree. The furnace experiments were carried out under a 99.999% Ar atmosphere to a
29 peak temperature of 1500 °C, at a heating rate of 10 °C/min. The wt% of reducing gases e.g. H₂, CO,
30 and hydrocarbons, and the temperature required for these gases to evolve was notably different for
31 each materials, but the respective maximum peaks of evolution of these gases corresponded well to
32 the maximum rate of mass loss. Furthermore, the off-gas analysis reveals torrefied grass contains
33 large amount of water and carbon dioxide which will be released at very low temperature, therefore
34 pre-treatment to the temperature of ~400 °C is necessary to produce chars with similar properties to
35 coal injected in HIsarna.

36

37 *Keywords:*

38 HIsarna technology

39 Biomass

40 Coal

41 Heating rate

42 Devolatilisation

43 Kinetic analysis

44

45 *** Corresponding author. Tel.: +44 (0)24 7652 4706**

46 **E-mail address: d.khasraw@warwick.ac.uk (D. Khasraw)**

47 **Postal address: WMG, University of Warwick, Coventry CV4 7AL, UK**

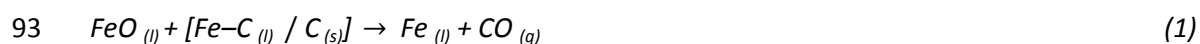
48 **1. Introduction**

49 Coal is the most widely used fossil fuel in the world, and it continues to dominate the energy supply
50 and the demand is still set to grow, particularly in developing countries despite international
51 environmental agreements. Stringent environmental legislations such as the compulsory target of
52 80-95% carbon dioxide (CO₂) emissions reduction by 2050 compared to the 1990 baseline, have
53 forced all industries into innovation and transformation [1]. Ironmaking is an energy intensive
54 process accounting for 4-7% of global CO₂ emissions alone [2]. With the strict environmental
55 legislation and recent signing of the Paris agreement, steel manufacturers are under continually
56 increasing pressure to reduce CO₂ emissions further to near net zero levels. Despite substantial
57 improvements concerning environmental performance, around a 50% reduction in CO₂ emissions
58 since 1990, it is believed a true step change in steel manufacturing technology is required. Current
59 technologies consisting of sintering, coke making and blast furnace (BF) ironmaking contribute to
60 approximately 90% of the CO₂ output from a blast furnace ironmaking-basic oxygen steelmaking
61 integrate steel plant [2]. Therefore significant efforts are now being funnelled into alternative
62 ironmaking technologies which promise the possibility to remove the necessity of coke making,
63 sintering and ultimately BF ironmaking. Several alternative ironmaking processes have been
64 commercialised or are under development, for example, commercially proven processes (COREX and
65 FINEX), ITmk3 process, coal-based or gas-based HYL process, coal-based MXCOL or gas-based
66 MIDREX, fluidised bed technologies (Cicored and circofer) and HIsarna technology [1, 4].

67 HIsarna technology is an alternative ironmaking process, which was developed under the European
68 Ultra-Low CO₂ steelmaking (ULCOS) research programme since 2004. The potential economic
69 benefits of low OPEX and CAPEX, its flexibility in raw materials (including scraps and wastes) and
70 fuels, the environmental benefits of significant reduction in CO₂ and other greenhouse gases and its
71 suitability for brownfield investment make the HIsarna process a prospective front runner as an

72 alternative to conventional BF. Hlsarna represents a new route of smelting reduction, which has
73 been developed by combining two known technologies of the Cyclone Converter Furnace (CCF) and
74 the Smelting Reduction Vessel (SRV) [3, 4]. Hlsarna has the ability to use a wider range of raw
75 materials and fuels in comparison to the conventional BF ironmaking. Hlsarna uses fine ores and
76 thermal coals, and eliminate the sintering/agglomeration and coke plants, which consequently
77 reduces the CO₂ emissions by up to 20% without carbon capture and storage (CCS) and potentially
78 80% with CCS [3, 5]. Partially substituting coking coal with thermal coal (pulverised coal injection),
79 renewable biomass and natural gas in the conventional BF has been achieved but the requirement
80 for burden support in the BF has set limitations on the use of these alternative fuels. However,
81 Hlsarna does not require burden support, therefore, it has great potential to fully substitute current
82 coking coal with other fuels including biomass, while maintaining process efficiency and productivity
83 [3].

84 The Hlsarna process begins with iron ore (and fluxing materials) and oxygen being pneumatically
85 injected into the CCF and hitting the wall of the CCF, where SRV off-gases are burning, as a result,
86 iron ore is pre-reduced by 10-20% and becomes partially molten. The partially reduced ore then
87 drips down along the wall under gravity at the temperature of approximately 1450 °C into the SRV
88 where the metal bath temperature is between 1400-1500 °C. Thermal coal is injected into the SRV
89 liquid metal which partly dissolves, adding carbon into the liquid metal to replenish that used in the
90 smelting reaction steps of the process [3, 5]. The smelting reactions are shown in equations (1) to
91 (3), (1) is an overall FeO reduction by carbon dissolved in the metal or solid char and (2) and (3) are
92 intermediate/alternative steps [6].



96 Replacement of coal with a carbon-neutral biomass in ironmaking offers great potential to reduce
97 reliance on non-renewable carbon sources in this major contributor to carbon dioxide emissions
98 from the steel industry. However, to maintain HIsarna's performance while substituting coal,
99 carbonisation of raw biomass is necessary to increase fixed carbon (C_{fix}) content and remove
100 moisture, oxygen and part of the volatile components, since existence of these components
101 decrease the energy content [7]. Different thermochemical conversion technologies can be used for
102 pre-treatment of the raw biomass to obtain chars with suitable properties for HIsarna. The pre-
103 treatment conditions as well as the type of raw biomass determine the chemical, physical, and
104 mechanical properties of the chars, which are necessary properties to produce chars which qualities
105 most closely resembles the thermal coal currently used in the HIsarna process to maintain process
106 efficiency and enable the technological shift in raw material use [5].

107 Once being injected into the smelting reduction vessel, the carbonaceous materials go through
108 complex reactions, two of which are devolatilisation and burning out of the carbon. Devolatilisation
109 happens first, and it continues to influence the solid carbon particles to the point when it is burnout
110 [8]. The gaseous products evolved during the heating process are light hydrocarbons (mainly CH_4 and
111 C_2H_6) which may crack into C and H_2 or react with the environment to form CO and H_2 or a mixture of
112 H_2 , H_2O , CO, and CO_2 , the balance of which will change the reducing environment and control other
113 parameters such as ignition, temperature and flame stability in the post combustion zone. As such
114 devolatilisation of carbonaceous materials used in HIsarna technology is a key phenomenon which
115 needs to be considered to achieve high efficiency [9]. While volatile matter is released the char
116 structure goes through significant changes e.g. particle break-up, softening and swelling, which is
117 strongly dependant on the chemical properties and reaction conditions such as heating rate,
118 temperature and pressure [8].

119 Biomass devolatilisation usually involves the thermal decomposition of three components namely
120 hemicellulose, cellulose, and lignin [10]. The process of decomposition for these components
121 proceeds in three stages: moisture desorption, active decay and passive decay. Moisture desorption

122 occurs at temperature < 150 °C. This is followed by active decay in which most of the volatile matter
123 is released at temperature between 200-500 °C, during this stage decomposition of hemicellulose
124 and cellulose takes place. Decomposition of lignin starts in active decay and continues to passive
125 decay at a very slow rate through the full temperature range of treatment [11]. Coal devolatilisation
126 proceeds through a similar thermal degradation process, starting with moisture desorption at
127 temperature < 150 °C and then degradation mobile and immobile phases occur at the temperatures
128 between 150-600 °C. This results in the formation of the aliphatic and aromatic tar components and
129 a number of light gases (e.g. H₂O, CO, CH₄ and CO₂). The final stage of thermal coal decomposition is
130 the breakup of heterocyclic compounds at temperature higher than 600 °C [12].

131 The literature contains studies on coal and biomass pyrolysis by using TGA [13-15], fixed-bed
132 reactors [16-18] and fluidized-bed reactors [19, 20]. TGA is the most common technique used to
133 study thermal decomposition and kinetic analysis of coal and biomass. Combining this equipment
134 with different analytic techniques, e.g. Fourier transform infrared spectrometry (FTIR) [21-24], gas
135 chromatography (GC) [25] and mass spectrometry (MS) [26-32] is quite common. Using these
136 techniques the gaseous products evolved during heat treatment can be investigated simultaneously
137 or afterwards to establish the mechanism for coal and biomass decomposition. TG-MS technique has
138 been applied because of its main advantage of being the on-line monitoring of evolving gases, which
139 can be used simultaneously with TG equipment to monitor the gas atmosphere during sample
140 decomposition. The effect of important parameters such as particle size, heating rate, holding time
141 and gas atmosphere have been studied using TGA. In addition there are numerous studies which
142 used simultaneous thermal/gas analysis to analyse evolved gases.

143 Much of the pyrolysis work done on gas evolution analysis has focused on determining the effect of
144 coal rank on the off-gas generated during thermal processing. Chinese coals with different grades
145 and different H/C atomic ratios have been studied using simultaneous gas analysis under an inert
146 atmosphere [26-28], and it was found that thermal decomposition and gas evolution behaviour of
147 coals are strongly dependent on temperature and the coal rank. This method has also been used to

148 study the effect of temperature and time [29] with regards to devolatilisation kinetics for different
149 types of biomass and coal/biomass blends [30, 31]. These researchers found that devolatilisation of
150 biomass is dependent on chemical properties including ash and volatile contents, temperature and
151 thermal treatment time. Additionally the off-gas of chitin biomass with various molecular structures
152 in an inert atmosphere was studied to determine the influence of zeolite catalysts on the utilization
153 of chitin biomass [32].

154 Although extensive research has been carried out on the devolatilisation behaviours for a number of
155 different coal and biomass, the research and development for the carbonaceous materials (coal and
156 biomass) for HIsarna technology is scarce, and also there is very limited information on direct
157 comparison between coal and biomass in term of devolatilisation. Much of the research done on
158 devolatilisation or gas evolution focused on the pyrolysis of coals and biomass using simultaneous
159 TGA-MS carried out with small sample size between (10-20) mg. Despite all the advantages of
160 simultaneously measurement such as real time analysis, qualitative and quantitative analysis but
161 small sample size may mean high level of uncertainty in the off-gas analysis due to side reactions. An
162 increase in the sample size in TGA can cause a temperature distribution problem and on the other
163 hand, TGA may struggle to handle heavy tar products if sample size increased. In this study a high
164 temperature vertical tube furnace coupled with a mass spectrometer is utilised to reliably study
165 larger samples with regards to their devolatilisation characteristics with an aim of attaining a more
166 accurate representation of gaseous product evolution from each sample under novel alternative
167 ironmaking technologies. This research aims to enable the selection of suitable fuel mix for the
168 HIsarna alternative ironmaking process.

169 **2. Materials and methods**

170 **2.1. Sample preparation**

171 Four coals and two biomass samples were tested in this study. Their proximate and ultimate analysis
172 are listed in Table 1. The four coal samples contain different levels of volatile matter (VM) from low

173 (8.63%, Coal C) to medium (16.00% Coal B and 22.18% Coal A) and high (36.00%, Coal D), while the
 174 two biomass samples are charcoal CC with 12.10% VM (a wood based pre-treated biomass) and
 175 torrefied grass TG with 63.60% VM (a grass-based torrefied material provided by OrangeGreen BV
 176 through Tata steel). Coal A and charcoal CC have already been used in Hlsarna process during the
 177 pilot plant trials and torrefied grass TG is another renewable source which may be considered for
 178 future trials. The samples were dried at 80 °C for 12 hours to ensure the removal of the free
 179 moisture and then crushed into small particles with the size range from 90 to 300 µm. The coal
 180 samples selected have different sulphur and ash contents that directly affect their reaction
 181 performance at high temperatures while biomass samples are generally much lower in sulphur and
 182 lower in ash contents.

183 Table 1. Proximate and ultimate values of the carbonaceous materials used in this study

	Coal A	Coal B	Coal C	Coal D	Charcoal CC	Torrefied Grass TG
Proximate Analysis wt% (db)						
Moisture/ % (ad)	8.87	7.11	1.24	1.30	4.56	4.40
Volatile Matter	22.18	16.00	8.63	33.00	12.10	63.60
Ash	8.80	10.00	4.41	7.20	1.80	4.40
Fixed Carbon (by difference)	69.02	74.00	86.96	59.80	86.10	32.00
Ultimate Analysis wt% (db)						
Carbon	81.91	83.60	86.97	80.30	89.4	57.60
Hydrogen	4.27	3.93	3.43	5.09	3.11	5.60
Nitrogen	2.19	1.07	1.20	1.50	0.57	0.29

Sulphur	0.24	0.78	0.86	0.89	0.06	0.09
Oxygen by (difference)	2.59	0.62	3.13	5.02	5.06	32.02

184 db - on a dry basis; ad - on an air dried.

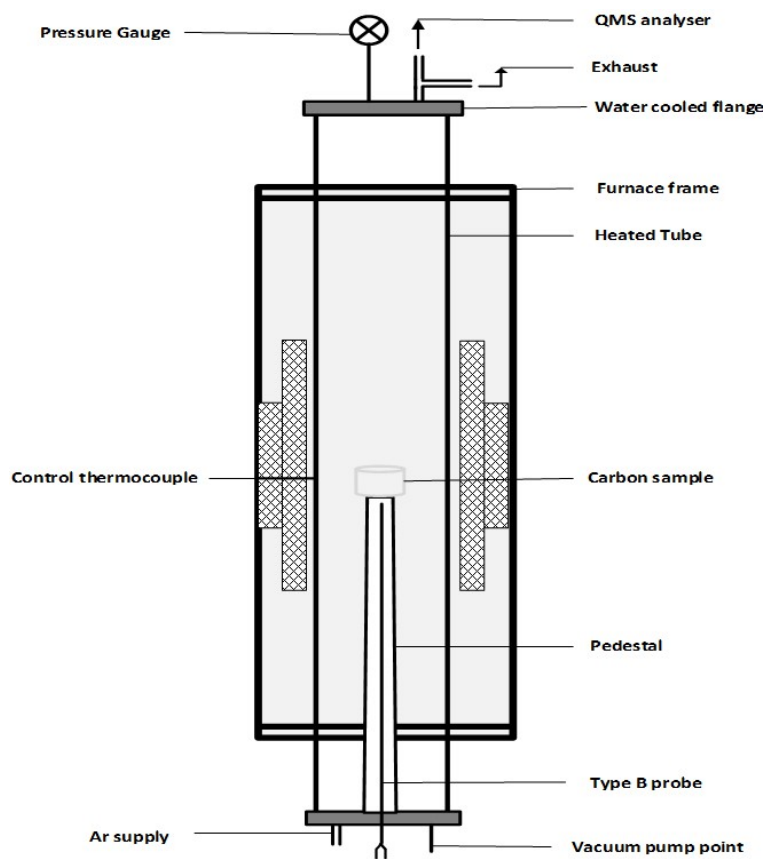
185 **2.2. Thermogravimetric analysis**

186 The mass loss due to devolatilisation under non-isothermal conditions was determined by using
187 thermogravimetric analysis (TGA) with a NETZSCH STA 449 instrument that has an analytical balance
188 sensitivity of ± 0.01 mg. A $20 \text{ mg} \pm 0.01$ sample was placed in an alumina crucible (height 4 mm x
189 diameter 6.8 mm). The alumina crucible with test sample was placed on a platinum stage, which has
190 a thermocouple located directly underneath to provide real temperature of the sample tested. All
191 the samples were heated in a high impurity (99.9999%) argon atmosphere at the flow rate of 50
192 ml/min. The mass loss due to volatile matter evolving was recorded from ambient temperature to
193 $1500 \text{ }^\circ\text{C}$, at the heating rates of 10, 20 and $30 \text{ }^\circ\text{C min}^{-1}$ respectively. To ensure the reliability and
194 reproducibility of the tests, preliminary tests have been carried out to define experimental
195 conditions, and the test for the same sample has been repeated three times to produce concordant
196 results.

197 **2.3. VTF-QMS gas analysis**

198 The gas analysis during devolatilisation was carried out using a Carbolite-Gero high temperature
199 vertical tube furnace with a recrystallized alumina tube (VTF-1700/50, internal diameter 88 mm x
200 length 1000 mm) shown in Figure 1. The furnace was coupled with a Hiden HPR 20 Quadrupole Mass
201 Spectrometer (QMS) to monitor gaseous products evolving from the samples. The VTF-QMS
202 combination allowed an increase in the sample weight to produce more representative volatile
203 measurements of the bulk material and reduce measurement uncertainties. The samples were
204 heated to $1500 \text{ }^\circ\text{C}$ in a high purity (99.9999%) argon atmosphere at the heating rate of $10 \text{ }^\circ\text{C/min}$
205 while the furnace exhaust was connected to the QMS through a heated capillary ($150 \text{ }^\circ\text{C}$) to monitor
206 gaseous products evolving from the samples and ensure no condensations occurred before the

207 ionization chamber. Each sample was weighed to be approximately 1.0 g and placed in an alumina
208 crucible on the alumina pedestal and lifted to the hot zone of the vertical tube furnace (VTF). The
209 tube was sealed, vacuumed using a standard rotary pump and then back filled with argon gas at a
210 flow rate of 300 ml min⁻¹ that carried gaseous products to the mass spectrometer (QMS). The argon
211 concentration was measured to be 99.7% before the furnace heating cycle started. The QMS was set
212 to measure readings of the following gases evolving from devolatilisation: N₂, O₂, CO, CO₂, Ar, H₂O,
213 H₂, CH₄ and C₂H₆. After the desired temperature was reached, the furnace cooled down at 5 °C/min
214 to room temperature in Ar atmosphere. Then the samples were taken out to weigh and analyse.



215

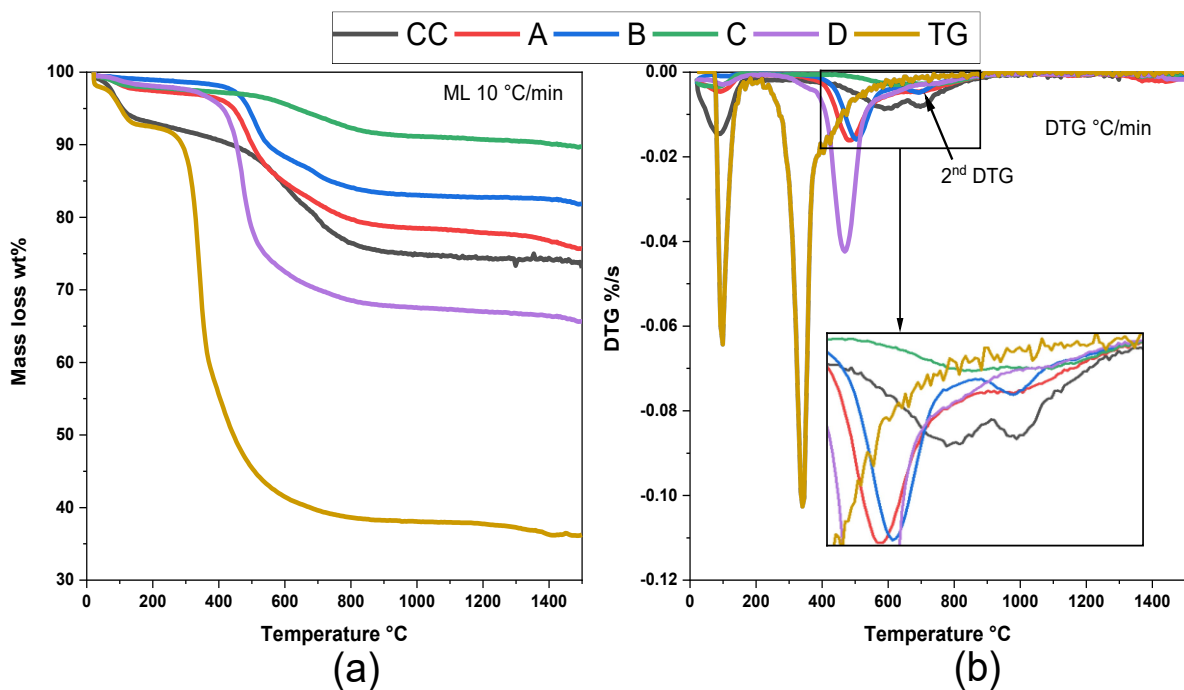
216 *Figure 1. Vertical tube furnace (VTF) setup with a mass spectrometry for devolatilisation study. The*
217 *quadrupole mass spectrometer (QMS) is connected to the gas sampling port.*

218 3. Results and discussion

219 3.1. TG-DTG analysis

220 The weight loss curves and derivative thermogravimetric (DTG) curves produced from the TGA tests
221 for the materials in Table 1, are shown in Figures 2a and 2b respectively. Figure 2a shows the weight
222 loss due to devolatilisation of the samples at the heating rate of 10 °C/min under argon atmosphere.
223 Slow weight loss begins for all four coal samples at the temperature of ~100 °C and continues to
224 ~180 °C, which is mainly associated with surface moisture loss. This is followed by rapid weight loss
225 due to the release of organic volatile matter, and the starting temperature of the release of organic
226 volatile matter depends on the volatile matter content of the coal sample. The weight loss curve
227 starts at lower temperature for coals with higher volatile matter but all the curves stabilise at the
228 temperature of around 650 °C regardless of the volatile matter contents. However, slow weight loss
229 to the temperature of 1500 °C was still notable, this could be from decomposition of materials with
230 a higher activation energy e.g. carbonyl and heterocyclic compounds, which subsequently leads to
231 CO and H₂ formation [9].

232

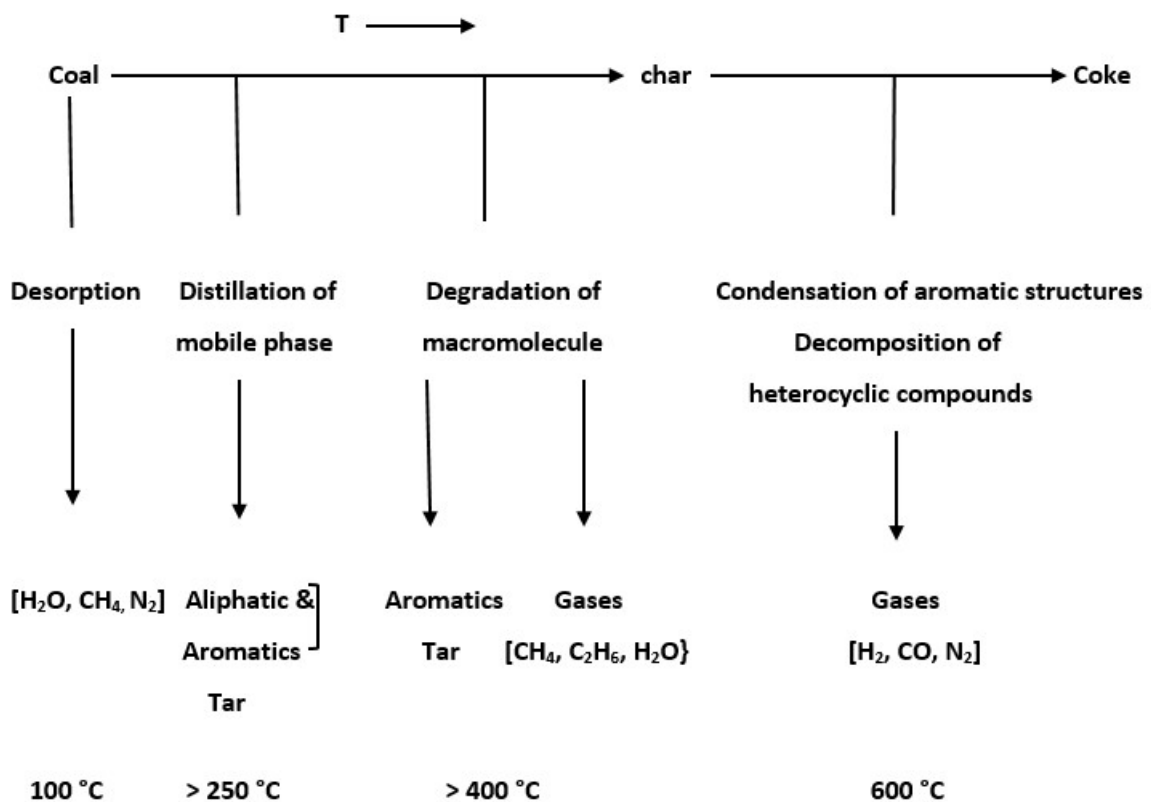


233

234 *Figure 2. (a) Mass loss curves and (b) DTG curves of the carbonaceous materials tested in the high*
235 *purity argon atmosphere at the heating rates of 10 °C/min from room temperature to 1500 °C.*

236 These thermal decomposition results for coal samples can be explained with the reported
 237 mechanisms of coal devolatilisation [33], such as the devolatilisation process proposed by van Heek
 238 and Hodek (Figure 3) [12]. Coal decomposition starts with desorption of moisture and some light
 239 gasses at the temperatures of ~ 100 °C. On continued heating to ~ 250 °C the mobile phase
 240 degradation occurs which leads to tar formation, in particular the aliphatic tar component. Then at
 241 the temperatures of 300 °C and higher, degradation of the immobile phase occurs which results in
 242 formation of the aromatic tar components and a number of light gases (e.g. H_2O , CO , CH_4 and CO_2)
 243 as shown in Figure 3 [12], which is evidenced by the experimental results shown in Figure 4 (section
 244 3.2). This is followed by decomposition of heterocyclic compounds at temperatures higher than 600
 245 °C producing N_2 , CO and H_2 gases.

246



247

248 *Figure 3. The main reactions occurring during the coal devolatilisation process [12]*

249 As shown in Figure 2, decomposition behaviour of biomass samples are different from the four coals
250 tested. The initial weight loss for both torrefied grass and charcoal starts at slightly lower
251 temperatures of ~ 80 °C and continues steadily to the temperature of 200 °C. After this a sharp
252 weight loss curve for torrefied grass occurs at temperatures from ~ 250 °C to 400 °C and the weight
253 loss continues slowly to 1500 °C. However, the second step of weight loss for charcoal starts at much
254 higher temperature of ~ 500 °C and continues to 1500 °C with a flatter weight loss curve that is
255 because of the pre-treatment of the starting material. Decomposition of hemicellulose is expected
256 to occur at the lower temperature range due to its random amorphous structure. The subsequent
257 decomposition of cellulose and lignin follows at higher temperatures as the materials are more
258 ordered and stronger bonded respectively. Biomass has a porous structure providing higher
259 adsorption potential than thermal coal, which is likely to allow large amounts of moisture and
260 carbon dioxide to be absorbed from the atmosphere. These absorbed components are weakly
261 bonded and evolve at the very low temperatures [34]. Cellulose is the main component responsible
262 for the second DTG peak, while lignin is the main component responsible for char formation.
263 However thermal degradation of lignin can start at low temperature at a very slow rate and
264 increases with the increase in temperature [35].

265 Figure 2b shows similar behaviour for coal samples, starting with the small peak at low temperature
266 due to desorption followed by a large single peak due to devolatilisation. The exception for this is
267 with coal B which has produced a clear secondary peak for devolatilisation, meaning coal B goes
268 through extra phase of decomposition. However torrefied grass and charcoal both produced larger
269 initial DTG peaks due to moisture loss followed by two devolatilisation peaks. There is one sharp
270 peak which starts at the temperature of ~ 250 °C and the second peak which is partially
271 superimposed on the late phase of the first peak for torrefied grass. This behaviour is linked to
272 decomposition of cellulose and lignin respectively, while charcoal produces two peaks at much
273 higher temperatures compared to torrefied grass which are from decomposition of lignin and agrees
274 with other researchers' findings on similar materials [15, 35].

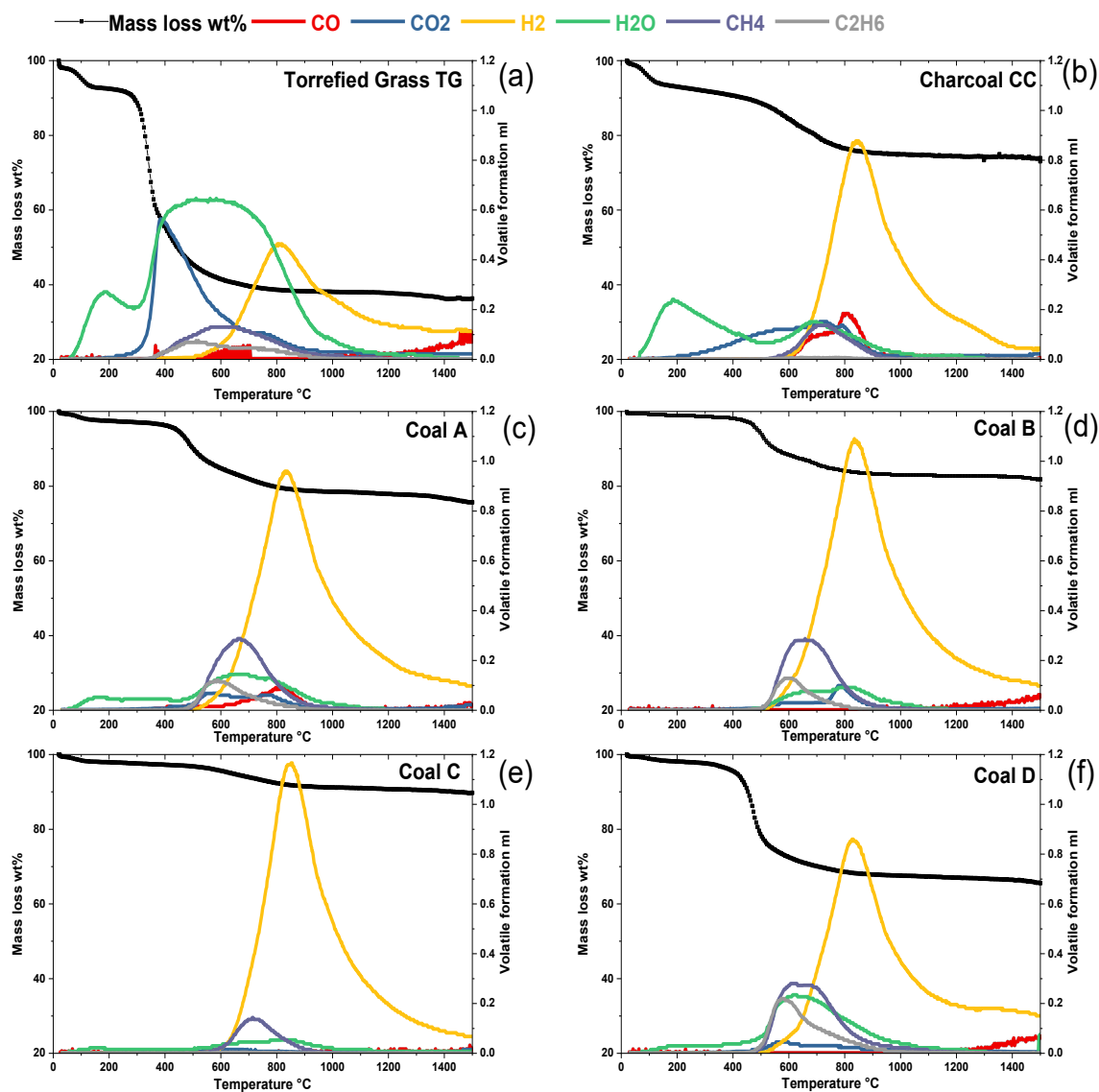
275 **3.2. Comparison of devolatilisation behaviours for different carbonaceous materials**

276 Various reactions occur simultaneously during devolatilisation upon heating, including break-up of
277 chemical bonds, vaporisation, and condensation or recombination [22]. Using a quadrupole mass
278 spectrometer (QMS) gaseous species evolved during heating process were measured continuously
279 up to the temperature of 1500 °C. Figure 4 shows the mass loss due to devolatilisation measured in
280 TGA tests against the normalized off-gas species measured in the VTF-QMS tests at the heating rate
281 of 10 °C/min for the two biomass and four coal samples.

282 Similar behaviour has been observed for all the samples that gas species detected at low
283 temperature of 100~200 °C were mainly H₂O, as the weight loss at low temperature is associated
284 with the loss of surface moisture. However, at this low temperature range, the weight loss of the
285 biomass samples was significantly higher than that of the coal samples measured, which is
286 confirmed by the amount of these gases detected. Devolatilisation continued with increasing
287 temperature, generating large amount of H₂O and CO₂ gas by biomass samples at temperature of
288 >300 °C while none or very small amount of CO₂ from coal samples was measured but still significant
289 amount of H₂O was produced. The amount of H₂O and CO₂ produced for torrefied grass during
290 heating was much higher than charcoal, as charcoal has already been pre-treated. However, the
291 amount of gas species generated by charcoal was still significantly higher than that from any of the
292 coal samples tested at similar temperatures, which could be due to higher oxygen content in the
293 charcoal, resulting in the oxidation of carbon and contributing to higher mass loss in charcoal.

294 The second region of weight loss is associated with the release of organic volatile matter, which
295 started at similar temperatures for all the samples but the gas species generated were different.
296 Both biomass samples started to generate H₂O and CO₂ at temperature > 300 °C, followed by the
297 release of hydrocarbons at temperature > 400 °C, and H₂ and CO at > 500 °C. The peaks for gases
298 generated in VTF-QMS tests spread over larger temperature range than those observed in TGA tests.
299 This is caused by the gas mixing in the VTF and the time require for evolved gases travelling from the

300 sample location to the detection of mass spectrometer. This travelling distance in the VTF tube gives
301 rise to the comparatively consistent delay for all devolatilisation peaks compared to the TGA results.
302 All the four coal samples tested were found to produce H₂O, CO₂, CH₄, C₂H₆ and H₂ at temperatures >
303 500 °C which corresponds to the region of mass loss in the TGA test results. The H₂O released at
304 temperature >150 °C is associated with the release of inherent moisture which presents in the
305 pore/capillaries of the carbonaceous materials and H₂O produced from decomposition of organic
306 components. It is also known that some H₂O exist as part of the crystal structure of inorganic
307 minerals which can contribute to H₂O formation at higher temperatures [36].

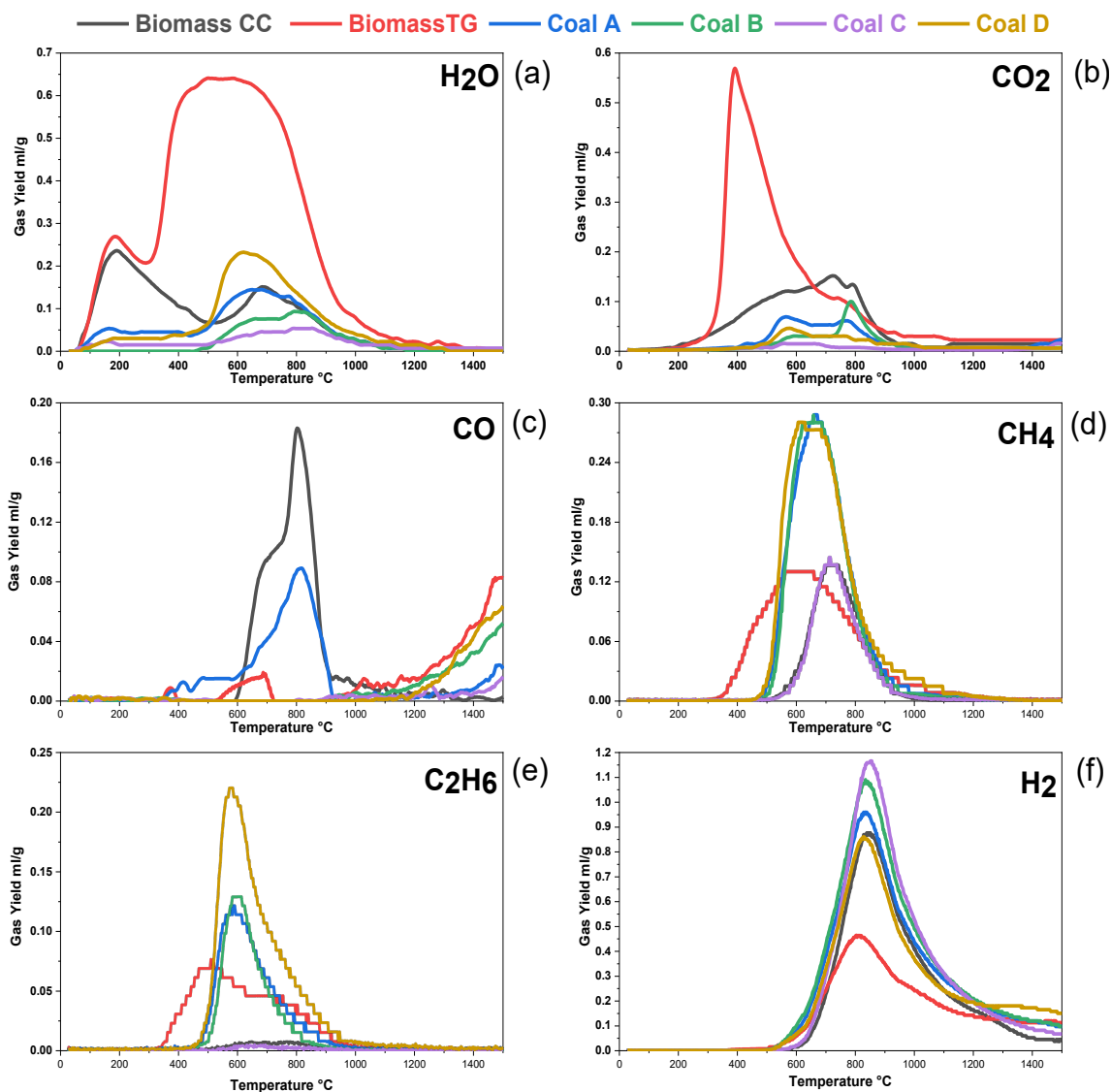


309

310 Figure 4. VTF-QMS for normalised gas species (CO , CO_2 , H_2 , H_2O , CH_4 , and C_2H_6) evolved against TGA
 311 mass loss during heating at the heating rate of $10^\circ\text{C}/\text{min}$ under argon atmosphere for (a) Torrefied
 312 grass (TG); (b) charcoal (CC), (c) coal A; (d) coal B; (e) coal C; (f) coal D.

313 The gas products evolved during the heating process are plotted in Figure 5, and some common
 314 phenomena can be observed for the biomass and coal samples. As it can be seen that both charcoal
 315 and torrefied grass samples produced larger amounts of H_2O at low temperature (100 to 200°C) than
 316 that of all coal samples. Each sample produced a peak for H_2O and CO_2 gas during the heating within
 317 the temperature range of 300 - 800°C , but the peak for both biomass samples was significantly

318 larger than those for the four coal samples. The sharp H₂O and CO₂ peaks for torrefied grass at the
319 temperature of 300-400 °C links well with the second sharp DTG peak for torrefied grass (shown in
320 Figure 2b) and presents the case that this is due to the release of H₂O and CO₂ from decomposition
321 of hemicellulose and cellulose at that temperature. Charcoal produced a flatter but wide peak of
322 H₂O and CO₂ which may be as a result of the sample already being pre-treated to similar
323 temperatures during the charcoal formation. Previous studies linked the amount and the
324 temperature required for the gas species to be produced to the chemical structure of the biomass
325 component used for the investigation [37]. Hemicellulose is higher in carboxyl content which results
326 in higher CO₂ yield, while cellulose contains carbonyl and carboxyl species which results in CO and
327 CO₂ product yield, and Lignin releases much more H₂ and CH₄ from cracking of aromatic rings and
328 methoxyl [15, 37].



330

331 *Figure 5. An off-gas analysis of (a) H₂O; (b) CO₂; (c) CO; (d) CH₄; (e) C₂H₆; and (f) H₂ evolved during*
 332 *VTF-QMS experiments.*

333 Torrefied grass was the only material which started to produce CH₄ and C₂H₆ at the temperatures
 334 under 400 °C, while all the other samples produced these gases at the temperature > 500 °C. Finally
 335 H₂ and CO formation happened in the higher temperature range which is linked to reactions that
 336 take place at higher activation energy [8, 38]. In addition, the thermal cracking of hydrocarbons is
 337 possible at temperature > 600 °C. The formation of CO and H₂ at high temperature is also linked to
 338 CH₄ reaction with CO₂ to form CO and H₂ [39]. Also hydrocarbons evolved at higher temperatures

339 may react with H₂O to form H₂ and some CO [30, 40] through the reaction schemes presented in
340 equations (4) and (5).



343 4. Kinetic analysis

344 4.1. The Kissinger–Akahira–Sunose method

345 The devolatilisation for carbonaceous materials is a complex process as several reactions occur
346 during thermal decomposition, which includes carbonizing and gas evolution simultaneously during
347 the heating process. For a better understanding of the devolatilisation process, many researchers
348 studied thermal decomposition of carbonaceous materials using TGA technique (which is the most
349 common technique) to measure the weight loss for kinetic analysis. The kinetic parameter obtain are
350 used to understand the complexity of the reaction and in modelling devolatilisation process to
351 predict the mass and energy balances. The devolatilisation mechanism can be described as
352 following: [22]

353 Raw carbonaceous materials \longrightarrow Volatile + Char

354 The devolatilisation conversion and apparent rate of reaction is calculated through equation (6):

$$355 \quad \frac{dx}{dt} = k(T)f(x) \quad (6)$$

356 The temperature dependent reaction rate constant $k(T)$ can be expressed by equation (7):

$$357 \quad k(T) = A e^{\left(\frac{E_x}{RT}\right)} \quad (7)$$

358 By combining equations (6) and (7) the overall reaction conversion rate can be expressed by
359 equation (8):

$$360 \quad \frac{dx}{dt} = A e^{\left(\frac{E_x}{RT}\right)} f(x) \quad (8)$$

361 where x , $\frac{dx}{dt}$, A , E_x , R , T and $f(x)$ denote the devolatilisation conversion degree, reaction conversion
362 rate, pre-exponential factor, activation energy, universal gas constant, temperature and reaction
363 function respectively.

364 The devolatilisation conversion degree(x) is defined by equation (9):

$$365 \quad x = \frac{mi - mt}{mi - mf} \quad (9)$$

366 where mi is the initial weight of the sample, mt is the instant weight of the sample at time t , and
367 mf is the final weight of the sample after the reaction.

368 The experiments are carried out using non-isothermal heating with a constant linear heating rate, β :

$$369 \quad \beta_i = \frac{dT}{dt} \quad (10)$$

370 where i represents the given heating rate being considered.

371 The following equation for reaction conversion rate can be obtained by equations (8) and (10):

$$372 \quad \frac{dx}{dT} = \frac{A}{\beta} e^{\left(\frac{E_x}{RT}\right)} f(x) \quad (11)$$

373 Equation (12) can be obtained by integrating equation (11) to represent the cumulative reaction
374 rate:

$$375 \quad g(x) = \int_0^x (f(x))^{-1} = \frac{A}{\beta} \int_0^T e^{\left(\frac{E_x}{RT}\right)} dT \quad (12)$$

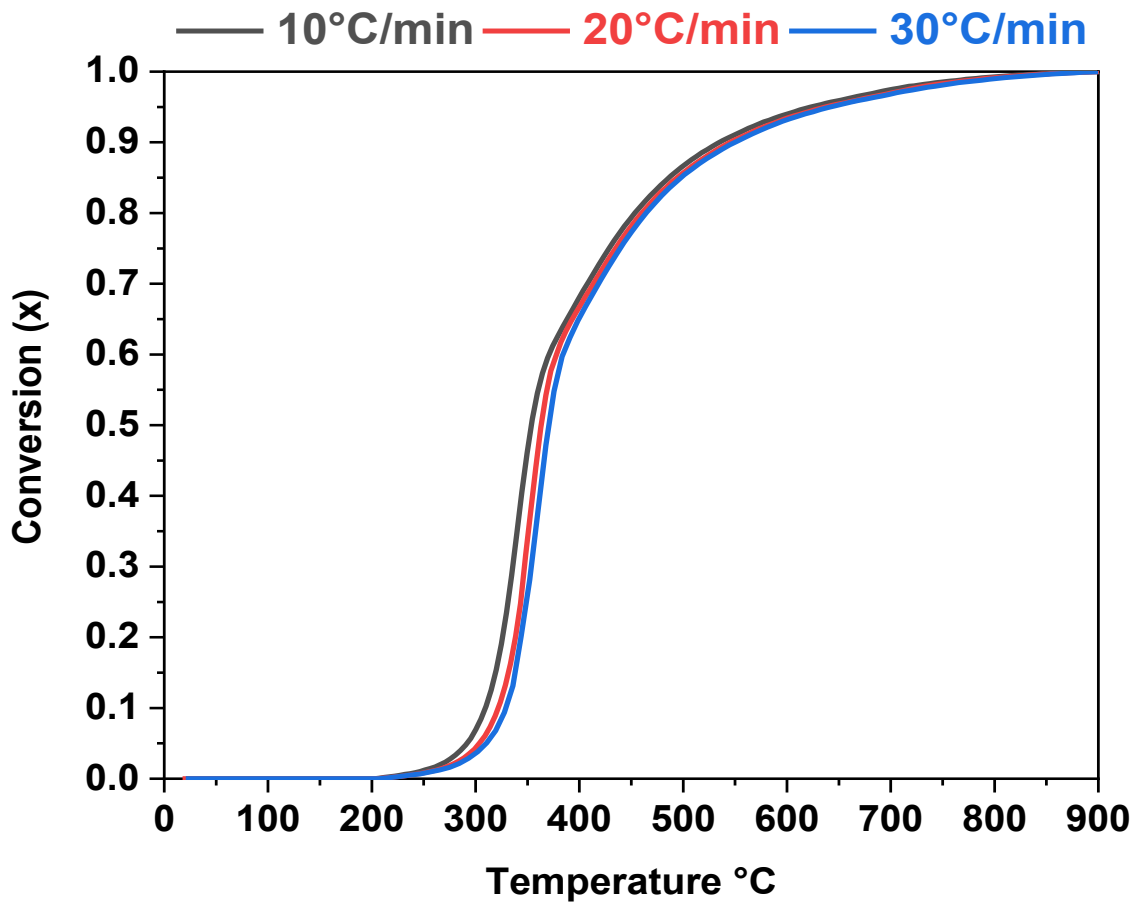
376 where $g(x) = \int_0^x (f(x))^{-1}$ is the integral form of the reaction model [32]. There are several
377 integral methods available which can be used to accurately estimate kinetic parameter. Among them
378 Kissinger–Akahira–Sunose (KAS) model is used by many researchers as a proven model, since the
379 kinetic parameters of a solid state reaction can be obtained without knowing the reaction
380 mechanism and also it is known to have high accuracy in estimating kinetic parameter [10, 31]. The
381 apparent activation energy (E_x) obtained by plotting natural logarithm of heating rate over

382 temperature square at a given value of conversion $\ln\left(\frac{\beta i}{T_{xi}^2}\right)$ versus $\frac{1000}{T_{xi}}$, which is represented by a
383 linear equation (13) for the KAS model for a given value of conversion, x , where the gradient is equal
384 to $-\frac{E_x}{R}$ [41].

$$385 \quad \ln\left(\frac{\beta i}{T_{xi}^2}\right) = \ln\left(\frac{A_x R x}{E_x g x}\right) - \frac{E_x}{RT_{xi}} \quad (13)$$

386 4.2. Kinetic analysis

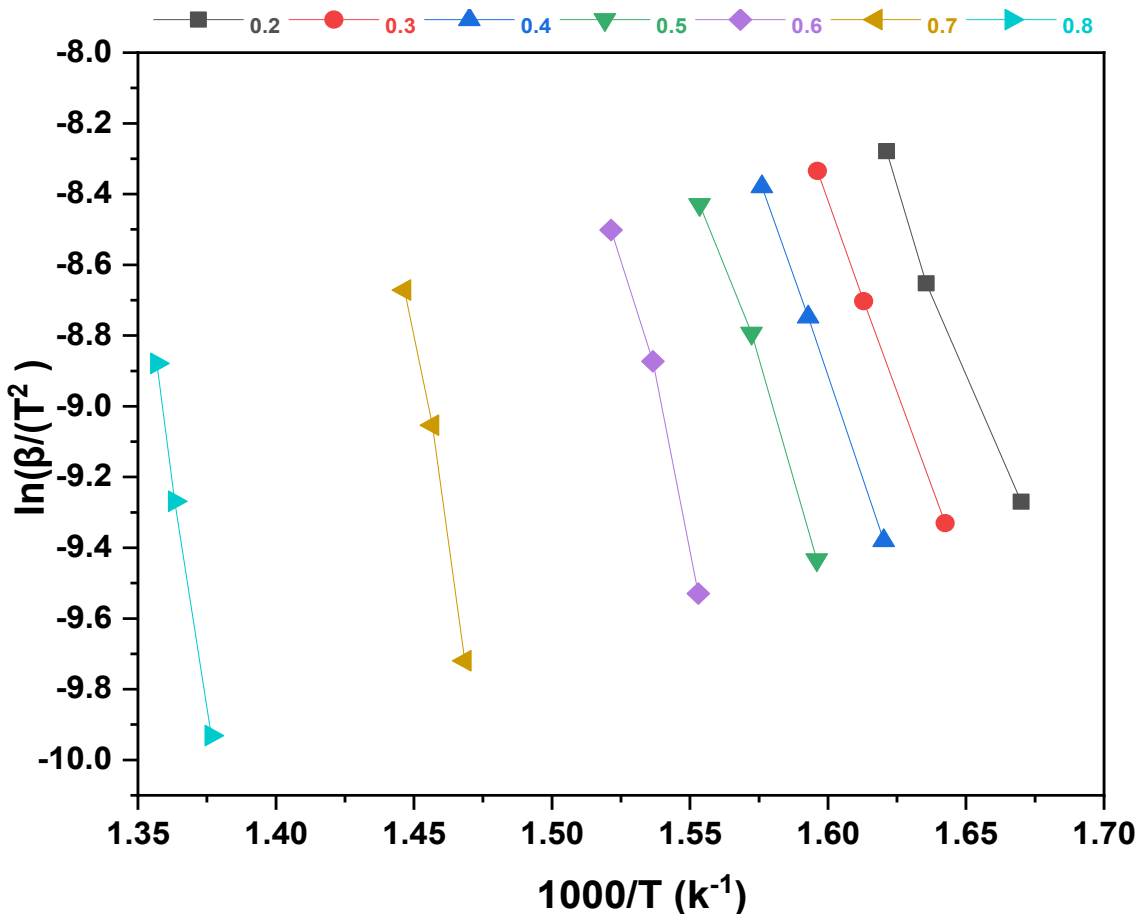
387 The results obtained from the TGA tests at three heating rates (10, 20, and 30 °C/min) are inputted
388 to a calculation according to the KAS method in order to calculate the activation energy (E_a) [10]. As
389 can be seen from off-gas analysis plots in Figure 5, at the temperature of < 200 °C the weight loss is
390 mostly related to surface moisture, with the devolatilisation process related to reducing gases
391 beginning at > 200 °C and then proceeding rapidly to 900 °C. So the devolatilisation conversion
392 degree (x) was calculated according to equation (9) for weight loss in the temperature range of 200-
393 900 °C for all carbonaceous materials tested. Figure 6 shows the devolatilisation conversion
394 degree(x) for torrefied grass (TG) as a function of temperature in TGA tests at the heating rates of
395 10, 20, and 30 °C/min.



396

397 *Figure 6. Extent of conversion curves for the devolatilisation process of torrefied grass (TG) as a*
 398 *function of temperature in TGA tests at different heating rates.*

399 The apparent activation energy from a plot of $\ln\left(\frac{\beta i}{T_{xi}^2}\right)$ versus $\frac{1000}{T_{xi}}$, for a given value of conversion
 400 (x) in the range of 0.2 to 0.8 is shown in Figure 7 for torrefied grass (TG). The average activation
 401 energy is calculated from the gradient equal to $-\frac{E_x}{R}$ and the correlation coefficients. R^2 values
 402 corresponding to the linear lines of best fit were in the range of 0.91 to 1.00 [33] showing good
 403 agreement.



404

405 *Figure 7. KAS plot of torrefied grass (TG) for different values of conversion to calculate the activation*
 406 *energy at different heating rates.*

407 Table 2 contains the calculated variables for all carbonaceous materials tested in this study. It is
 408 seen that the apparent activation energy was not the same for all conversion degrees, which
 409 confirms the occurrence of different reactions at different temperatures during the experiment.

410 Charcoal has quite high and stable E_a values throughout, and the value does not change a lot with
 411 the change in conversion degree probably because of the effects of pre-treatment on this material.

412 Torrefied grass behaved differently, starting with a low E_a value at a low conversion degree and
 413 increasing linearly with an increase of conversion. This may correspond to low E_a values for
 414 decomposition of the remaining hemicellulose and cellulose but higher E_a values for lignin

415 decomposition. Coal A shows a similar behaviour to charcoal with quite stable high E_a values, while

416 coal B which contains medium volatile matter content has low stable E_a values. Coal C has low E_a

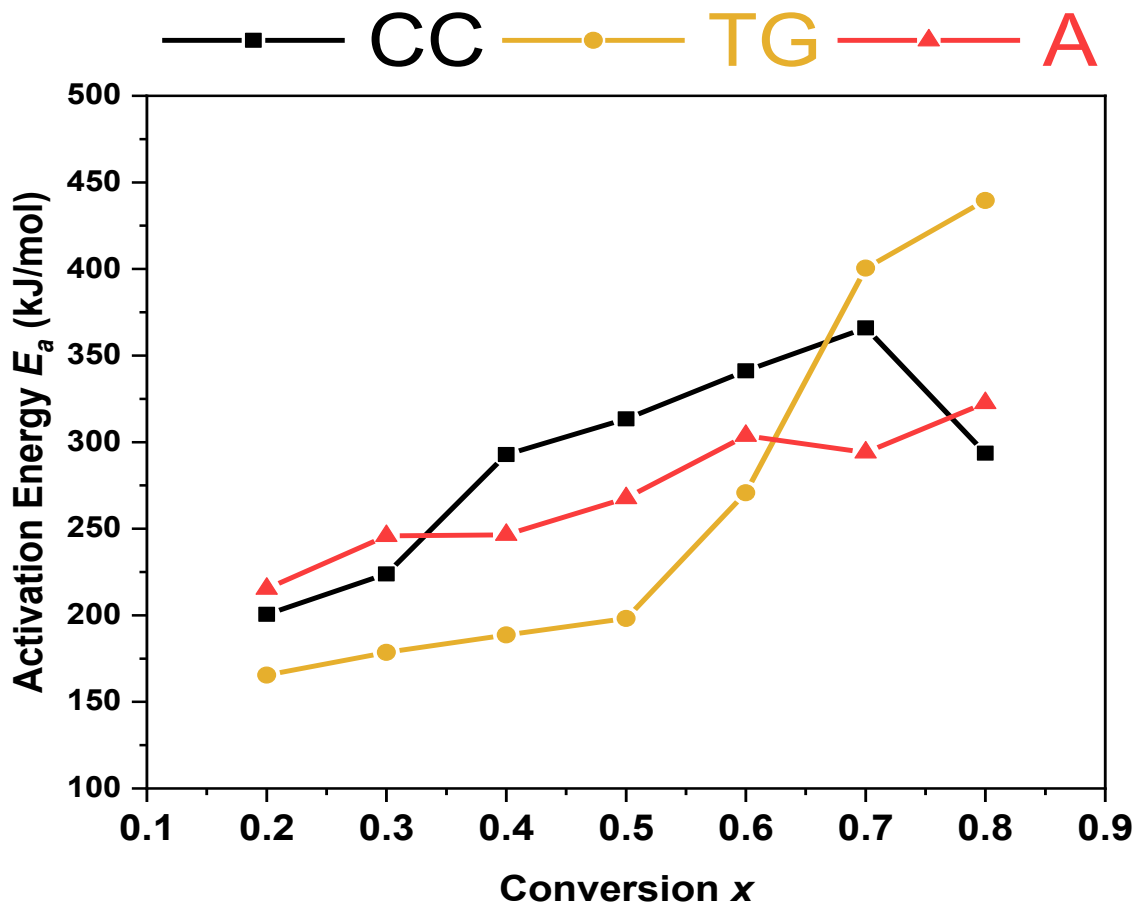
417 value at low conversion degree and increases linearly with an increase in conversion. Coal D starts
 418 with low E_a value at low conversion degree and increases linearly with an increase in conversion
 419 degrees up to 0.6 conversion, and then there is a significant increase in the values at conversion
 420 degrees of 0.7 and 0.8. This behaviour may be influenced by error in the method since the difference
 421 for conversion degrees at different heating rates are not very large, which is seen in Figure 6.

422 *Table 2. Activation energy E_a values in kJ/mol obtained for different carbon sources by using KAS, R^2*
 423 *corresponding to linear fittings*

Conversion (x)	CC		TG		A		B		C		D	
	E_a	R^2	E_a	R^2	E_a	R^2	E_a	R^2	E_a	R^2	E_a	R^2
0.2	201	0.99	165	0.99	215	1.00	183	0.96	77	0.95	192	0.99
0.3	224	1.00	179	1.00	246	1.00	194	0.97	120	0.93	242	0.99
0.4	293	1.00	189	1.00	247	1.00	197	0.97	154	0.93	278	1.00
0.5	313	1.00	198	0.99	268	1.00	193	0.96	185	0.95	311	1.00
0.6	341	1.00	271	0.98	304	1.00	180	0.91	219	0.94	390	0.99
0.7	366	1.00	400	0.99	294	1.00	169	0.92	264	0.95	650	0.98
0.8	294	1.00	440	1.00	323	1.00	173	0.95	335	0.95	1897	95.00
Average E_a	290		263		271		184		194		566	

424 These kinetic models assume the same reactions occurring at a specific conversion degree for
 425 different materials but as it can be observed from Figure 4 that multiple reactions take place at
 426 different temperatures. Therefore it is difficult to make accurate comparison between different
 427 carbon materials. This means the reaction mechanism can change during the devolatilisation
 428 process, therefore E_a is dependent on conversion and the average value of E_a can be estimated as a
 429 function of conversion. Kinetic analysis showed charcoal, torrefied grass and coal A (already injected

430 in Hlsarna trials) have similar average activation energy values (290, 263 and 271 kJ/mol
 431 respectively). Since decomposition of the carbon materials consists of multiple chemical reactions,
 432 the E_a value may change depending on the reactions taking place at specific conversion degree. It
 433 can be noticed in Figure 8 that the value of E_a increases with an increase in conversion.



434

435 *Figure 8. Activation energy E_a as a function of the conversion degree for charcoal (CC), torrefied gas*
 436 *(TG) and Coal A.*

437 The increase in E_a for torrefied grass is notably larger. This is because at low conversion levels very
 438 large amounts of weakly bonded components evolved e.g. H_2O and CO_2 shown in Figure 4 (a),
 439 therefore less energy is required for them to be removed. Charcoal starts with lower E_a at
 440 conversion degrees of 0.2 and 0.3 compared to coal A, but coal A has lower E_a at conversion degree
 441 of 0.4 - 0.7. As can be seen in Figures 4 (b) and (c) charcoal produces larger amount of CO_2 at low
 442 temperature where coal A produces more of the other volatiles e.g. CH_4 , C_2H_6 and H_2 at lower

443 temperature which confirms the differences in the E_a values. Based on off-gas analysis and kinetic
444 values charcoal with current properties is the more likely source of biomass which can replace
445 thermal coal in Hlsarna technology, however material handling and pre-treatment may need to be
446 re-considered to optimise its use in the process.

447 **5. Comparison of carbonaceous materials for Hlsarna process**

448 The results of this study indicate that different reactions take place during specific conversion
449 degree for different carbon materials, therefore devolatilisation is affected by the material
450 properties which in turn is linked to volatile mater content. There has been similarities in
451 devolatilisation behaviour (such as devolatilisation temperature), which is essential for smelting
452 reduction vessel in Hlsarna process. Biomass samples produced significantly larger amount of H₂O
453 and CO₂ at low temperatures, however, coal samples produce more CH₄, C₂H₆ and H₂.

454 Despite the pre-treatment of biomass charcoal samples, this study showed that there is still
455 significant weight loss (release of H₂O) at low temperatures because H₂O is absorbed from
456 atmosphere due to their porous structure of the charcoal. Torrefied grass releases a large amount of
457 H₂O and CO₂ at the temperature between 300-400 °C due to its high oxygen potential. These gases
458 and H₂O releasing at lower temperatures can cause temperature drop in the Hlsarna furnace which
459 needs heat compensation and due to high O₂ level much more carbon material may be needed. To
460 avoid these problems and utilise torrefied grass efficiently, a pre-treatment at the temperature of up
461 to 400 °C in inert atmosphere is necessary to reduce the oxygen content and produce bio-chars with
462 similar chemical properties to thermal coal currently used in Hlsarna. To complete this process heat
463 sources from other parts of the steel plant can be utilized to keep the “green” credentials of
464 biomass, the gasses and tars released in the pre-treatment process can be used to generate heat
465 and power for Hlsarna process.

466 Because of the porous structure of biomass carbon sources (e.g. charcoal), material handling needs
467 to be different to avoid H₂O absorption from atmosphere which is evidence in the test results. It may

468 need to consider pre-heating biomass to the temperature of ~200 °C before injection to remove all
469 H₂O and other oxide impurities from biomass surface to maintain HIsarna process efficiency. Further
470 studies may be required to investigate the effect of H₂O content in carbonaceous materials on
471 HIsarna process such as materials handling and heat balance.

472 **6. Conclusions**

473 In order to enable the selection of suitable fuel mix in the novel HIsarna ironmaking process, four
474 coals with notable differences in volatile matter content along with two biomass samples sourced
475 from wood and grass origins were investigated in this study. The following conclusions can be
476 obtained.

- 477 • The wt% of reducing gases e.g. H₂, CO, and hydrocarbons, and the temperature required for
478 these gases to evolve was notably different for all the carbonaceous materials tested in this
479 study, but the respective maximum peaks of evolution of these gases corresponded well to the
480 maximum rate of mass loss.
- 481 • The off-gas analysis reveals torrefied grass contains large amount of water and carbon dioxide
482 which will be released at very low temperature, therefore pre-treatment to the temperature of
483 ~400 °C is necessary to produce chars with similar properties to coal injected in HIsarna.
- 484 • The change of reactivation energy E_a as a function of conversion degree is determined, which is
485 linked to different reactions at different temperatures.
- 486 • Materials handling needs to be different for biomass (compared to thermal coal) to avoid H₂O
487 absorption.

488 **Acknowledgement**

489 DK would like to thank Tata Steel Nederland Technology BV for providing PhD scholarship (Reference
490 Number: COL1421/GIPS03241) to carry out this research. ZL would like to appreciate the funding
491 from EPSRC under the grant number EP/N011368/1. The authors appreciate Tata Steel HIsarna team
492 for fruitful discussions and providing samples. DK also would like to thank Dr. Ian Moore at Material

493 Processing Institute for providing coal C and coal D samples, and Tata Steel IJmuiden would like to
494 acknowledge OrangeGreen BV for providing the torrefied grass sample.

495 **References:**

- 496 [1] Hasanbeigi, A., Arens, M. & Price, L. Alternative emerging ironmaking technologies for energy-
497 efficiency and carbon dioxide emissions reduction : A technical review. *Renewable and*
498 *Sustainable Energy Reviews* 33, 645-658 (2014).
- 499 [2] Suopajarvi, H. et al. Use of biomass in integrated steelmaking – Status quo, future needs and
500 comparison to other low-CO₂ steel production technologies. *Appl. Energy* 213, 384–407
501 (2018).
- 502 [3] Abdul Quader, M., Ahmed, S., Dawal, S. Z. & Nukman, Y. Present needs, recent progress and
503 future trends of energy-efficient Ultra-Low Carbon Dioxide (CO₂) Steelmaking (ULCOS)
504 program. *Renew. Sustain. Energy Rev.* 55, 537–549 (2016).
- 505 [4] Meijer, K., Zeilstra, C., Teerhuis, C., Ouwehand, M. & Van Der Stel, J. Developments in
506 alternative ironmaking. *Trans. Indian Inst. Met.* (2013). doi:10.1007/s12666-013-0309-z
- 507 [5] Meijer, K., Guenther, C. & Dry, R. J. Hlsarna Pilot Plant Project. *InSteelCon* 1–5 (2011).
- 508 [6] TEASDALE, S. and HAYES, P., 2005. Observations of the Reduction of FeO from Slag by
509 Graphite, Coke and Coal Char. *ISIJ International*, 45(5), pp.634-641.
- 510 [7] Boggelen, J., Meijer, K., Zeilstra, C., Hage, H. and Broersen, P. (2019). Hlsarna - Demonstrating
511 low CO₂ ironmaking at pilot scale.
- 512 [8] Yu, J., Lucas, J. and Wall, T., 2007. Formation of the structure of chars during devolatilisation
513 of pulverized coal and its thermoproperties: A review. *Progress in Energy and Combustion*
514 *Science*, 33(2), pp.135-170.
- 515 [9] Chen, L., Zeng, C., Guo, X., Mao, Y., Zhang, Y., Zhang, X., Li, W., Long, Y., Zhu, H., Eiteneer, B.
516 and Zamansky, V. (2010). Gas evolution kinetics of two coal samples during rapid pyrolysis.
517 *Fuel Processing Technology*, 91(8), pp.848-852.

- 518 [10] Slopiecka, K., Bartocci, P. and Fantozzi, F. (2012). Thermogravimetric analysis and kinetic study
519 of poplar wood pyrolysis. *Applied Energy*, 97, pp.491-497.
- 520 [11] Gašparovič, L., Koreňová, Z. and Jelemenský, Ľ. (2010). Kinetic study of wood chips
521 decomposition by TGA. *Chemical Papers*, 64(2).
- 522 [12] van Heek, K. and Hodek, W. (1994). Structure and pyrolysis behaviour of different coals and
523 relevant model substances. *Fuel*, 73(6), pp.886-896.
- 524 [13] Anca-Couce, A. and Obernberger, I. (2016). Application of a detailed biomass pyrolysis kinetic
525 scheme to hardwood and softwood torrefaction. *Fuel*, 167, pp.158-167.
- 526 [14] Dwivedi, K., Chatterjee, P., Karmakar, M. and Pramanick, A. (2019). Pyrolysis characteristics
527 and kinetics of Indian low rank coal using thermogravimetric analysis. *International Journal of
528 Coal Science & Technology*, 6(1), pp.102-112.
- 529 [15] Ren, S.; Lei, H.; Wang, L.; Bu, Q.; Chen, S.; Wu, J. Thermal behaviour and kinetic study for
530 woody biomass torrefaction and torrefied biomass pyrolysis by TGA. *Biosyst. Eng.* 2013, 116,
531 420–426, doi:10.1016/j.biosystemseng.2013.10.003.
- 532 [16] Liu, J., Jiang, X., Shen, J. and Zhang, H. (2014). Pyrolysis of superfine pulverized coal. Part 1.
533 Mechanisms of methane formation. *Energy Conversion and Management*, 87, pp.1027-1038.
- 534 [17] Ferdous, D., Dalai, A., Bej, S., Thring, R. and Bakhshi, N. (2001). Production of H₂ and medium
535 Btu gas via pyrolysis of lignins in a fixed-bed reactor. *Fuel Processing Technology*, 70(1), pp.9-
536 26.
- 537 [18] Yan, X., Che, D. and Xu, T. (2005). Effect of rank, temperatures and inherent minerals on
538 nitrogen emissions during coal pyrolysis in a fixed bed reactor. *Fuel Processing Technology*,
539 86(7), pp.739-756.
- 540 [19] Heidari, A., Stahl, R., Younesi, H., Rashidi, A., Troeger, N. and Ghoreyshi, A. (2014). Effect of
541 process conditions on product yield and composition of fast pyrolysis of *Eucalyptus grandis* in
542 fluidized bed reactor. *Journal of Industrial and Engineering Chemistry*, 20(4), pp.2594-2602.

- 543 [20] Zhang, X., Dong, L., Zhang, J., Tian, Y. and Xu, G. (2011). Coal pyrolysis in a fluidized bed
544 reactor simulating the process conditions of coal topping in CFB boiler. *Journal of Analytical
545 and Applied Pyrolysis*, 91(1), pp.241-250.
- 546 [21] Biagini, E., Barontini, F. and Tognotti, L. (2006). Devolatilisation of Biomass Fuels and Biomass
547 Components Studied by TG/FTIR Technique. *Industrial & Engineering Chemistry Research*,
548 45(13), pp.4486-4493.
- 549 [22] Xu, R., Zhang, J., Wang, G., Zuo, H., Liu, Z., Jiao, K., Liu, Y. and Li, K. (2016). Devolatilisation
550 Characteristics and Kinetic Analysis of Lump Coal from China COREX3000 Under High
551 Temperature. *Metallurgical and Materials Transactions B*, 47(4), pp.2535-2548.
- 552 [23] Chen, D., Liu, D., Zhang, H., Chen, Y. and Li, Q. (2015). Bamboo pyrolysis using TG–FTIR and a
553 lab-scale reactor: Analysis of pyrolysis behavior, product properties, and carbon and energy
554 yields. *Fuel*, 148, pp.79-86.
- 555 [24] Bassilakis, R., Carangelo, R. and Wójtowicz, M. (2001). TG-FTIR analysis of biomass pyrolysis.
556 *Fuel*, 80(12), pp.1765-1786.
- 557 [25] Zhang, X., Dong, L., Zhang, J., Tian, Y. and Xu, G. (2011). Coal pyrolysis in a fluidized bed
558 reactor simulating the process conditions of coal topping in CFB boiler. *Journal of Analytical
559 and Applied Pyrolysis*, 91(1), pp.241-250.
- 560 [26] Han, F., Meng, A., Li, Q. and Zhang, Y. (2016). Thermal decomposition and evolved gas analysis
561 (TG-MS) of lignite coals from Southwest China. *Journal of the Energy Institute*, 89(1), pp.94-
562 100.
- 563 [27] Li, x., Matuschek, G., Herrera, M., Wang, H. and Kettrup, A. (2002). Investigation of pyrolysis of
564 Chinese coals using thermal analysis/mass spectrometry. *Thermal Analysis and Calorimetry*,
565 71, pp.601–612.
- 566 [28] Arenillas, A., Rubiera, F. and Pis, J. (1999). Simultaneous thermogravimetric–mass
567 spectrometric study on the pyrolysis behaviour of different rank coals. *Journal of Analytical
568 and Applied Pyrolysis*, 50(1), pp.31-46.

- 569 [29] Wannapeera, J., Fungtammasan, B. and Worasuwanarak, N. (2011). Effects of temperature
570 and holding time during torrefaction on the pyrolysis behaviors of woody biomass. *Journal of*
571 *Analytical and Applied Pyrolysis*, 92(1), pp.99-105.
- 572 [30] Jayaraman, K., Kok, M. and Gokalp, I. (2017). Thermogravimetric and mass spectrometric (TG-
573 MS) analysis and kinetics of coal-biomass blends. *Renewable Energy*, 101, pp.293-300.
- 574 [31] El-Tawil, A., Ökvist, L., M. Ahmed, H. and Björkman, B. (2019). Devolatilisation Kinetics of
575 Different Types of Bio-Coals Using Thermogravimetric Analysis. *Metals*, 9(2), p.168.
- 576 [32] Qiao, Y., Chen, S., Liu, Y., Sun, H., Jia, S., Shi, J., Pedersen, C., Wang, Y. and Hou, X. (2015).
577 Pyrolysis of chitin biomass: TG–MS analysis and solid char residue characterization.
578 *Carbohydrate Polymers*, 133, pp.163-170.
- 579 [33] Borah, R., Ghosh, P. and Rao, P. (2011). A review on devolatilisation of coal in fluidized bed.
580 *International Journal of Energy Research*, 35(11), pp.929-963.
- 581 [34] Yang, H., Yan, R., Chen, H., Zheng, C., Lee, D. and Liang, D. (2006). In-Depth Investigation of
582 Biomass Pyrolysis Based on Three Major Components: Hemicellulose, Cellulose and Lignin.
583 *Energy & Fuels*, 20(1), pp.388-393.
- 584 [35] Yang, H., Yan, R., Chen, H., Lee, D. and Zheng, C. (2007). Characteristics of hemicellulose,
585 cellulose and lignin pyrolysis. *Fuel*, 86(12-13), pp.1781-1788.
- 586 [36] Zhu, Q., 2014. *Coal Sampling And Analsis Standards*. [online] Usea.org. Available at:
587 <https://usea.org/sites/default/files/042014_Coal%20sampling%20and%20analysis%20standards_ccc235.pdf> [Accessed 25 June 2020].
- 589 [37] Werner, K., Pommer, L. and Broström, M. (2014). Thermal decomposition of hemicelluloses.
590 *Journal of Analytical and Applied Pyrolysis*, 110, pp.130-13.
- 591 [38] Yang, H., Yan, R., Chen, H., Lee, D., Liang, D. and Zheng, C. (2006). Mechanism of Palm Oil
592 Waste Pyrolysis in a Packed Bed. *Energy & Fuels*, 20(3), pp.1321-1328.
- 593 [39] Halmann, M., 2018. *Chemical Fixation Of Carbon Dioxidemethods For Recycling CO2 Into*
594 *Useful Products*. Boca Raton: Chapman and Hall/CRC.

- 595 [40] Basile, A., Centi, G., De Falco, M. and Iaquaniello, G., 2019. Catalysis, Green Chemistry And
596 Sustainable Energy. 1st ed. San Diego: Elsevier, pp.284-288.
- 597 [41] Kissinger, H. (1956). Variation of peak temperature with heating rate in differential thermal
598 analysis. Journal of Research of the National Bureau of Standards, 57(4), p.217

1 Devolatilisation Characteristics of Coal and Biomass with Respect to 2 Temperature and Heating Rate for Hlsarna Alternative Ironmaking 3 Process

4 Darbaz Khasraw ^{a,*}, Stephen Spooner ^a, Hans Hage ^b, Koen Meijer ^b, Zushu Li ^a

5 ^aWMG, University of Warwick, Coventry, UK

6 ^bTata Steel IJmuiden, The Netherlands

7

8 HIGHLIGHTS

- 9 • Devolatilisation behaviours of different carbon sources investigated for Hlsarna alternative
10 ironmaking process.
- 11 • Maximum peaks of evolved gases from VTF-QMS corresponded well to DTG curves.
- 12 • The kinetic parameters for coal and biomass samples were determined.
- 13 • Biomass pre-treatment temperature suggested to produce chars with similar properties to coal
14 injected in Hlsarna.

15 **Abstract:** Hlsarna process offers a novel low CO₂ emission alternative to the blast furnace for
16 primary iron production. This new smelting ironmaking technology is flexible in raw material usage
17 such as the substitution of biomass for coal as a reductant. Reduction is conducted through multiple
18 mechanisms within the smelting vessel including gaseous reaction products from thermal
19 decomposition of volatile matters reacting directly with iron oxide containing slags and injected iron
20 ore. In this study, four coals with notable differences in volatile matter content along with two
21 biomass samples sourced from wood and grass origins were investigated for the selection of suitable
22 fuel mix. Thermogravimetric analysis (TGA) was used to measure the weight loss of the

23 carbonaceous materials and a vertical tube furnace coupled with a quadrupole mass spectrometer
24 (VTF-QMS) was employed for off-gas analysis during the devolatilisation. During TGA tests the
25 samples were heated under a 99.9999 % argon atmosphere to 1500 °C at three different heating
26 rates to investigate the kinetics of thermal decomposition for these materials. Through use of the
27 Kissinger– Akahira–Sonuse model an average activation energy was determined as a function of the
28 conversion degree. The furnace experiments were carried out under a 99.999% Ar atmosphere to a
29 peak temperature of 1500 °C, at a heating rate of 10 °C/min. The wt% of reducing gases e.g. H₂, CO,
30 and hydrocarbons, and the temperature required for these gases to evolve was notably different for
31 each materials, but the respective maximum peaks of evolution of these gases corresponded well to
32 the maximum rate of mass loss. Furthermore, the off-gas analysis reveals torrefied grass contains
33 large amount of water and carbon dioxide which will be released at very low temperature, therefore
34 pre-treatment to the temperature of ~400 °C is necessary to produce chars with similar properties to
35 coal injected in HIsarna.

36

37 *Keywords:*

38 HIsarna technology

39 Biomass

40 Coal

41 Heating rate

42 Devolatilisation

43 Kinetic analysis

44

45 *** Corresponding author. Tel.: +44 (0)24 7652 4706**

46 **E-mail address: d.khasraw@warwick.ac.uk (D. Khasraw)**

47 **Postal address: WMG, University of Warwick, Coventry CV4 7AL, UK**

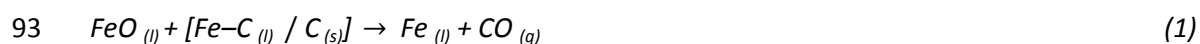
48 **1. Introduction**

49 Coal is the most widely used fossil fuel in the world, and it continues to dominate the energy supply
50 and the demand is still set to grow, particularly in developing countries despite international
51 environmental agreements. Stringent environmental legislations such as the compulsory target of
52 80-95% carbon dioxide (CO₂) emissions reduction by 2050 compared to the 1990 baseline, have
53 forced all industries into innovation and transformation [1]. Ironmaking is an energy intensive
54 process accounting for 4-7% of global CO₂ emissions alone [2]. With the strict environmental
55 legislation and recent signing of the Paris agreement, steel manufacturers are under continually
56 increasing pressure to reduce CO₂ emissions further to near net zero levels. Despite substantial
57 improvements concerning environmental performance, around a 50% reduction in CO₂ emissions
58 since 1990, it is believed a true step change in steel manufacturing technology is required. Current
59 technologies consisting of sintering, coke making and blast furnace (BF) ironmaking contribute to
60 approximately 90% of the CO₂ output from a blast furnace ironmaking-basic oxygen steelmaking
61 integrate steel plant [2]. Therefore significant efforts are now being funnelled into alternative
62 ironmaking technologies which promise the possibility to remove the necessity of coke making,
63 sintering and ultimately BF ironmaking. **Several alternative ironmaking processes have been**
64 **commercialised or are under development, for example, commercially proven processes (COREX and**
65 **FINEX), ITmk3 process, coal-based or gas-based HYL process, coal-based MXCOL or gas-based**
66 **MIDREX, fluidised bed technologies (Cicored and circofer) and HIsarna technology [1, 4].**

67 HIsarna technology is an alternative ironmaking process, which was developed under the European
68 Ultra-Low CO₂ steelmaking (ULCOS) research programme since 2004. **The potential economic**
69 **benefits of low OPEX and CAPEX, its flexibility in raw materials (including scraps and wastes) and**
70 **fuels, the environmental benefits of significant reduction in CO₂ and other greenhouse gases and its**
71 **suitability for brownfield investment make the HIsarna process a prospective front runner as an**

72 **alternative to conventional BF**. Hlsarna represents a new route of smelting reduction, which has
73 been developed by combining two known technologies of the Cyclone Converter Furnace (CCF) and
74 the Smelting Reduction Vessel (SRV) [3, 4]. Hlsarna has the ability to use a wider range of raw
75 materials and fuels in comparison to the conventional **BF** ironmaking. Hlsarna uses fine ores and
76 thermal coals, and eliminate the sintering/agglomeration and coke plants, which consequently
77 reduces the CO₂ emissions by up to 20% without carbon capture and storage (CCS) and potentially
78 80% with CCS [3, 5]. Partially substituting coking coal with thermal coal (pulverised coal injection),
79 renewable biomass and natural gas in the conventional **BF** has been achieved but the requirement
80 for burden support in the **BF** has set limitations on the use of these alternative fuels. However,
81 Hlsarna does not require burden support, therefore, it has great potential to fully substitute current
82 coking coal with other fuels including biomass, while maintaining process efficiency and productivity
83 [3].

84 The Hlsarna process begins with iron ore (and fluxing materials) and oxygen being **pneumatically**
85 injected into the CCF **and hitting the wall of the CCF**, where **SRV** off-gases are burning, as a result,
86 iron ore is pre-reduced by 10-20% and becomes partially molten. The partially reduced ore then
87 **drips down along the wall** under gravity at the temperature of approximately 1450 °C into the SRV
88 where the metal bath temperature is between 1400-1500 °C. Thermal coal is injected into the SRV
89 liquid metal which partly dissolves, adding carbon into the liquid metal to replenish that used in the
90 smelting reaction steps of the process [3, 5]. The smelting reactions are shown in equations (1) to
91 (3), (1) is an overall FeO reduction by carbon dissolved in the metal or solid char and (2) and (3) are
92 intermediate/alternative steps [6].



96 Replacement of coal with a carbon-neutral biomass in ironmaking offers great potential to reduce
97 reliance on non-renewable carbon sources in this major contributor to carbon dioxide emissions
98 from the steel industry. However, to maintain HIsarna's performance while substituting coal,
99 carbonisation of raw biomass is necessary to increase fixed carbon (C_{fix}) content and remove
100 moisture, oxygen and part of the volatile components, since existence of these components
101 decrease the energy content [7]. Different thermochemical conversion technologies can be used for
102 pre-treatment of the raw biomass to obtain chars with suitable properties for HIsarna. The pre-
103 treatment conditions as well as the type of raw biomass determine the chemical, physical, and
104 mechanical properties of the chars, which are necessary properties to produce chars which qualities
105 most closely resembles the thermal coal currently used in the HIsarna process to maintain process
106 efficiency and enable the technological shift in raw material use [5].

107 Once being injected into the smelting reduction vessel, the carbonaceous materials go through
108 complex reactions, two of which are devolatilisation and burning out of the carbon. Devolatilisation
109 happens first, and it continues to influence the solid carbon particles to the point when it is burnout
110 [8]. The gaseous products evolved during the heating process are light hydrocarbons (mainly CH_4 and
111 C_2H_6) which may crack into C and H_2 or react with the environment to form CO and H_2 or a mixture of
112 H_2 , H_2O , CO, and CO_2 , the balance of which will change the reducing environment and control other
113 parameters such as ignition, temperature and flame stability in the post combustion zone. As such
114 devolatilisation of carbonaceous materials used in HIsarna technology is a key phenomenon which
115 needs to be considered to achieve high efficiency [9]. While volatile matter is released the char
116 structure goes through significant changes e.g. particle break-up, softening and swelling, which is
117 strongly dependant on the chemical properties and reaction conditions such as heating rate,
118 temperature and pressure [8].

119 Biomass devolatilisation usually involves the thermal decomposition of three components namely
120 hemicellulose, cellulose, and lignin [10]. The process of decomposition for these components
121 proceeds in three stages: moisture desorption, active decay and passive decay. Moisture desorption

122 occurs at temperature < 150 °C. This is followed by active decay in which most of the volatile matter
123 is released at temperature between 200-500 °C, during this stage decomposition of hemicellulose
124 and cellulose takes place. Decomposition of lignin starts in active decay and continues to passive
125 decay at a very slow rate through the full temperature range of treatment [11]. Coal devolatilisation
126 proceeds through a similar thermal degradation process, starting with moisture desorption at
127 temperature < 150 °C and then degradation mobile and immobile phases occur at the temperatures
128 between 150-600 °C. This results in the formation of the aliphatic and aromatic tar components and
129 a number of light gases (e.g. H₂O, CO, CH₄ and CO₂). The final stage of thermal coal decomposition is
130 the breakup of heterocyclic compounds at temperature higher than 600 °C [12].

131 The literature contains studies on coal and biomass pyrolysis by using TGA [13-15], fixed-bed
132 reactors [16-18] and fluidized-bed reactors [19, 20]. TGA is the most common technique used to
133 study thermal decomposition and kinetic analysis of coal and biomass. Combining this equipment
134 with different analytic techniques, e.g. Fourier transform infrared spectrometry (FTIR) [21-24], gas
135 chromatography (GC) [25] and mass spectrometry (MS) [26-32] is quite common. Using these
136 techniques the gaseous products evolved during heat treatment can be investigated simultaneously
137 or afterwards to establish the mechanism for coal and biomass decomposition. TG-MS technique has
138 been applied because of its main advantage of being the on-line monitoring of evolving gases, which
139 can be used simultaneously with TG equipment to monitor the gas atmosphere during sample
140 decomposition. The effect of important parameters such as particle size, heating rate, holding time
141 and gas atmosphere have been studied using TGA. In addition there are numerous studies which
142 used simultaneous thermal/gas analysis to analyse evolved gases.

143 Much of the pyrolysis work done on gas evolution analysis has focused on determining the effect of
144 coal rank on the off-gas generated during thermal processing. Chinese coals with different grades
145 and different H/C atomic ratios have been studied using simultaneous gas analysis under an inert
146 atmosphere [26-28], and it was found that thermal decomposition and gas evolution behaviour of
147 coals are strongly dependent on temperature and the coal rank. This method has also been used to

148 study the effect of temperature and time [29] with regards to devolatilisation kinetics for different
149 types of biomass and coal/biomass blends [30, 31]. These researchers found that devolatilisation of
150 biomass is dependent on chemical properties including ash and volatile contents, temperature and
151 thermal treatment time. Additionally the off-gas of chitin biomass with various molecular structures
152 in an inert atmosphere was studied to determine the influence of zeolite catalysts on the utilization
153 of chitin biomass [32].

154 Although extensive research has been carried out on the devolatilisation behaviours for a number of
155 different coal and biomass, the research and development for the carbonaceous materials (coal and
156 biomass) for HIsarna technology is scarce, and also there is very limited information on direct
157 comparison between coal and biomass in term of devolatilisation. Much of the research done on
158 devolatilisation or gas evolution focused on the pyrolysis of coals and biomass using simultaneous
159 TGA-MS carried out with small sample size between (10-20) mg. Despite all the advantages of
160 simultaneously measurement such as real time analysis, qualitative and quantitative analysis but
161 small sample size may mean high level of uncertainty in the off-gas analysis due to side reactions. An
162 increase in the sample size in TGA can cause a temperature distribution problem and on the other
163 hand, TGA may struggle to handle heavy tar products if sample size increased. In this study a high
164 temperature vertical tube furnace coupled with a mass spectrometer is utilised to reliably study
165 larger samples with regards to their devolatilisation characteristics with an aim of attaining a more
166 accurate representation of gaseous product evolution from each sample under novel **alternative**
167 ironmaking technologies. This research aims to enable the selection of suitable fuel mix for the
168 HIsarna alternative ironmaking process.

169 **2. Materials and methods**

170 **2.1. Sample preparation**

171 Four coals and two biomass samples were tested in this study. Their proximate and ultimate analysis
172 are listed in Table 1. The four coal samples contain different levels of volatile matter (VM) from low

173 (8.63%, Coal C) to medium (16.00% Coal B and 22.18% Coal A) and high (36.00%, Coal D), while the
 174 two biomass samples are charcoal CC with 12.10% VM (a wood based pre-treated biomass) and
 175 torrefied grass TG with 63.60% VM (a grass-based torrefied material provided by OrangeGreen BV
 176 through Tata steel). Coal A and charcoal CC have already been used in Hlsarna process during the
 177 pilot plant trials and torrefied grass TG is another renewable source which may be considered for
 178 future trials. The samples were dried at 80 °C for 12 hours to ensure the removal of the free
 179 moisture and then crushed into small particles with the size range from 90 to 300 µm. The coal
 180 samples selected have different sulphur and ash contents that directly affect their reaction
 181 performance at high temperatures while biomass samples are generally much lower in sulphur and
 182 lower in ash contents.

183 Table 1. Proximate and ultimate values of the carbonaceous materials used in this study

	Coal A	Coal B	Coal C	Coal D	Charcoal CC	Torrefied Grass TG
Proximate Analysis wt% (db)						
Moisture/ % (ad)	8.87	7.11	1.24	1.30	4.56	4.40
Volatile Matter	22.18	16.00	8.63	33.00	12.10	63.60
Ash	8.80	10.00	4.41	7.20	1.80	4.40
Fixed Carbon (by difference)	69.02	74.00	86.96	59.80	86.10	32.00
Ultimate Analysis wt% (db)						
Carbon	81.91	83.60	86.97	80.30	89.4	57.60
Hydrogen	4.27	3.93	3.43	5.09	3.11	5.60
Nitrogen	2.19	1.07	1.20	1.50	0.57	0.29

Sulphur	0.24	0.78	0.86	0.89	0.06	0.09
Oxygen by (difference)	2.59	0.62	3.13	5.02	5.06	32.02

184 db - on a dry basis; ad - on an air dried.

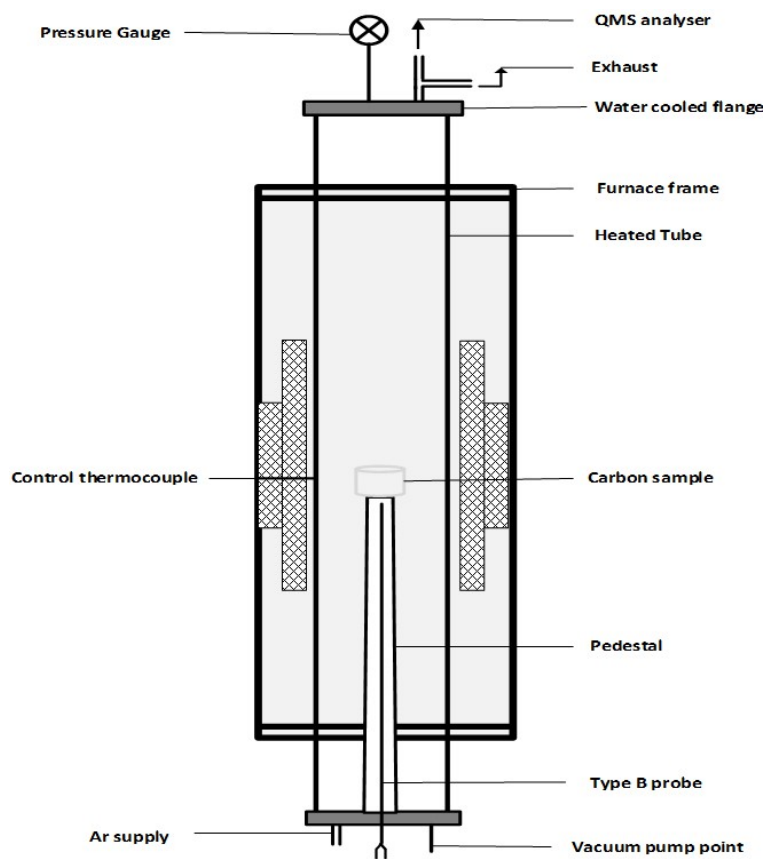
185 2.2. Thermogravimetric analysis

186 The mass loss due to devolatilisation under non-isothermal conditions was determined by using
187 thermogravimetric analysis (TGA) with a NETZSCH STA 449 instrument that has an analytical balance
188 sensitivity of ± 0.01 mg. A $20 \text{ mg} \pm 0.01$ sample was placed in an alumina crucible (height 4 mm x
189 diameter 6.8 mm). The alumina crucible with test sample was placed on a platinum stage, which has
190 a thermocouple located directly underneath to provide real temperature of the sample tested. All
191 the samples were heated in a high impurity (99.9999%) argon atmosphere at the flow rate of 50
192 ml/min. The mass loss due to volatile matter evolving was recorded from ambient temperature to
193 $1500 \text{ }^\circ\text{C}$, at the heating rates of 10, 20 and $30 \text{ }^\circ\text{C min}^{-1}$ respectively. To ensure the reliability and
194 reproducibility of the tests, preliminary tests have been carried out to define experimental
195 conditions, and the test for the same sample has been repeated three times to produce concordant
196 results.

197 2.3. VTF-QMS gas analysis

198 The gas analysis during devolatilisation was carried out using a Carbolite-Gero high temperature
199 vertical tube furnace with a recrystallized alumina tube (VTF-1700/50, internal diameter 88 mm x
200 length 1000 mm) shown in Figure 1. The furnace was coupled with a Hiden HPR 20 Quadrupole Mass
201 Spectrometer (QMS) to monitor gaseous products evolving from the samples. The VTF-QMS
202 combination allowed an increase in the sample weight to produce more representative volatile
203 measurements of the bulk material and reduce measurement uncertainties. The samples were
204 heated to $1500 \text{ }^\circ\text{C}$ in a high purity (99.9999%) argon atmosphere at the heating rate of $10 \text{ }^\circ\text{C/min}$
205 while the furnace exhaust was connected to the QMS through a heated capillary ($150 \text{ }^\circ\text{C}$) to monitor
206 gaseous products evolving from the samples and ensure no condensations occurred before the

207 ionization chamber. Each sample was weighed to be approximately 1.0 g and placed in an alumina
208 crucible on the alumina pedestal and lifted to the hot zone of the vertical tube furnace (VTF). The
209 tube was sealed, vacuumed using a standard rotary pump and then back filled with argon gas at a
210 flow rate of 300 ml min⁻¹ that carried gaseous products to the mass spectrometer (QMS). The argon
211 concentration was measured to be 99.7% before the furnace heating cycle started. The QMS was set
212 to measure readings of the following gases evolving from devolatilisation: N₂, O₂, CO, CO₂, Ar, H₂O,
213 H₂, CH₄ and C₂H₆. After the desired temperature was reached, the furnace cooled down at 5 °C/min
214 to room temperature in Ar atmosphere. Then the samples were taken out to weigh and analyse.



215

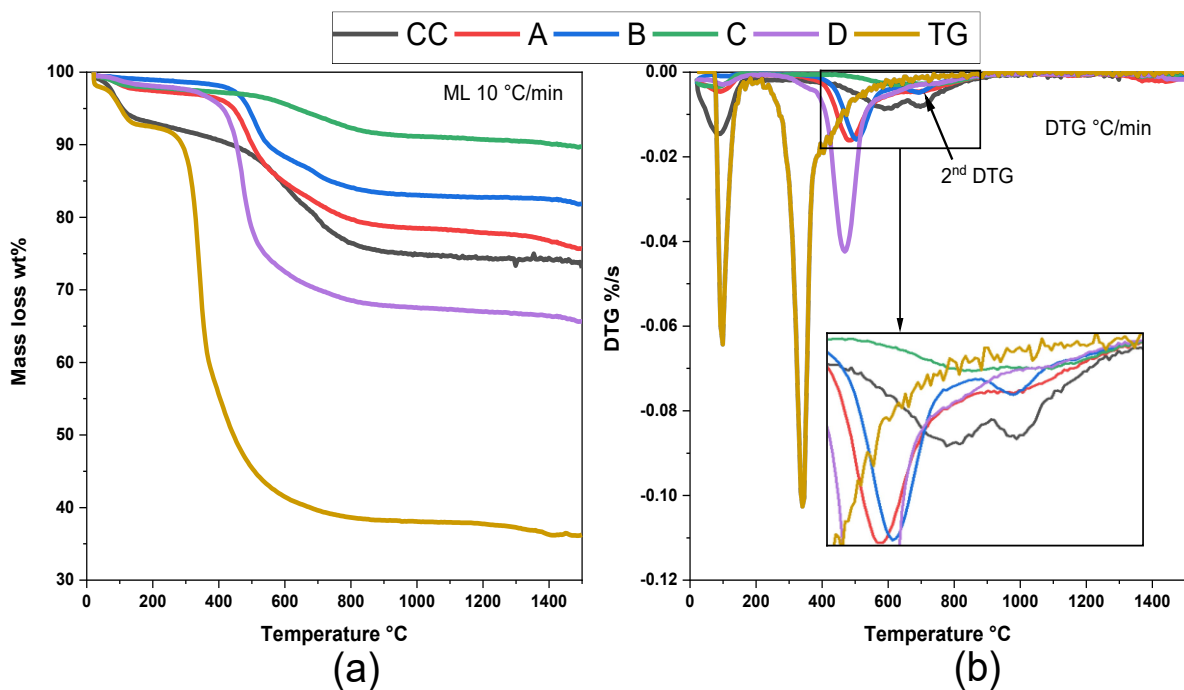
216 *Figure 1. Vertical tube furnace (VTF) setup with a mass spectrometry for devolatilisation study. The*
217 *quadrupole mass spectrometer (QMS) is connected to the gas sampling port.*

218 3. Results and discussion

219 3.1. TG-DTG analysis

220 The weight loss curves and derivative thermogravimetric (DTG) curves produced from the TGA tests
 221 for the materials in Table 1, are shown in Figures 2a and 2b respectively. Figure 2a shows the weight
 222 loss due to devolatilisation of the samples at the heating rate of 10 °C/min under argon atmosphere.
 223 Slow weight loss begins for all four coal samples at the temperature of ~100 °C and continues to
 224 ~180 °C, which is mainly associated with surface moisture loss. This is followed by rapid weight loss
 225 due to the release of organic volatile matter, and the starting temperature of the release of organic
 226 volatile matter depends on the volatile matter content of the coal sample. The weight loss curve
 227 starts at lower temperature for coals with higher volatile matter but all the curves stabilise at the
 228 temperature of around 650 °C regardless of the volatile matter contents. However, slow weight loss
 229 to the temperature of 1500 °C was still notable, this could be from decomposition of materials with
 230 a higher activation energy e.g. carbonyl and heterocyclic compounds, which subsequently leads to
 231 CO and H₂ formation [9].

232

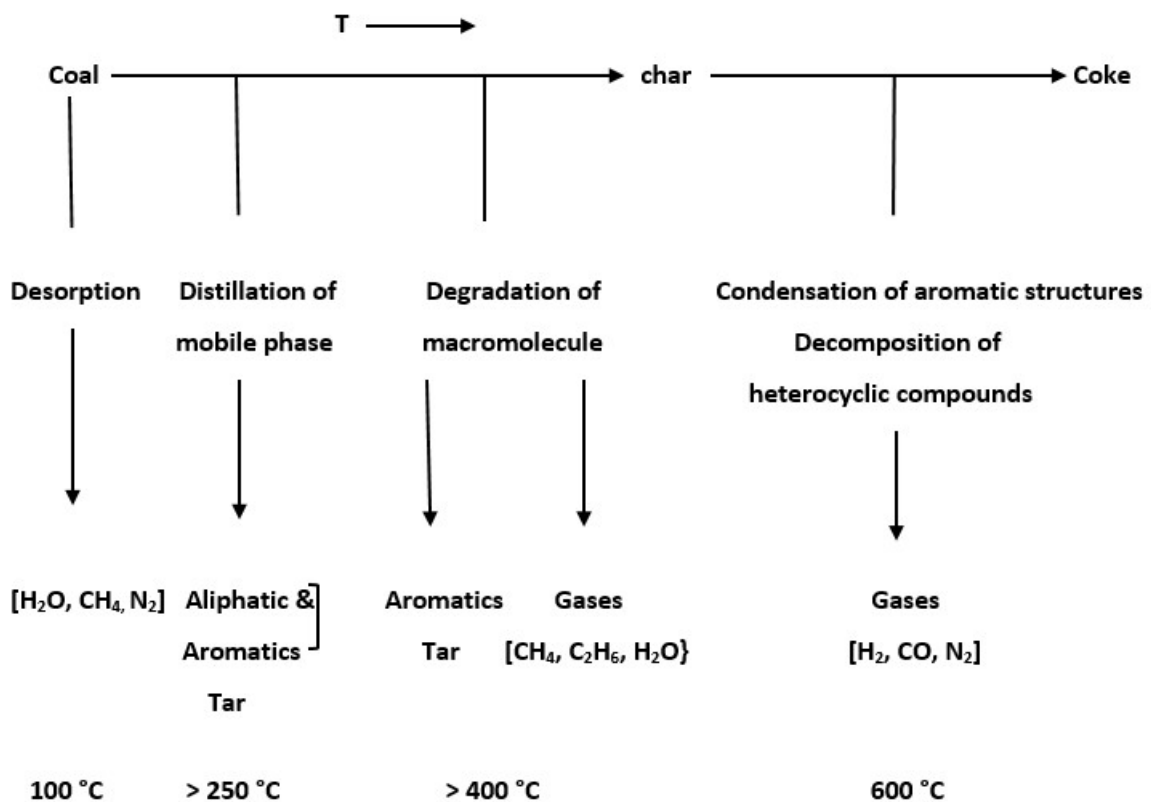


233

234 *Figure 2. (a) Mass loss curves and (b) DTG curves of the carbonaceous materials tested in the high*
 235 *purity argon atmosphere at the heating rates of 10 °C/min from room temperature to 1500 °C.*

236 These thermal decomposition results for coal samples can be explained with the reported
 237 mechanisms of coal devolatilisation [33], such as the devolatilisation process proposed by van Heek
 238 and Hodek (Figure 3) [12]. Coal decomposition starts with desorption of moisture and some light
 239 gasses at the temperatures of ~100 °C. On continued heating to ~250 °C the mobile phase
 240 degradation occurs which leads to tar formation, in particular the aliphatic tar component. Then at
 241 the temperatures of 300 °C and higher, degradation of the immobile phase occurs which results in
 242 formation of the aromatic tar components and a number of light gases (e.g. H₂O, CO, CH₄ and CO₂)
 243 as shown in Figure 3 [12], which is evidenced by the experimental results shown in Figure 4 (section
 244 3.2). This is followed by decomposition of heterocyclic compounds at temperatures higher than 600
 245 °C producing N₂, CO and H₂ gases.

246



247

248 *Figure 3. The main reactions occurring during the coal devolatilisation process [12]*

249 As shown in Figure 2, decomposition behaviour of biomass samples are different from the four coals
250 tested. The initial weight loss for both torrefied grass and charcoal starts at slightly lower
251 temperatures of ~ 80 °C and continues steadily to the temperature of 200 °C. After this a sharp
252 weight loss curve for torrefied grass occurs at temperatures from ~ 250 °C to 400 °C and the weight
253 loss continues slowly to 1500 °C. However, the second step of weight loss for charcoal starts at much
254 higher temperature of ~ 500 °C and continues to 1500 °C with a flatter weight loss curve that is
255 because of the pre-treatment of the starting material. Decomposition of hemicellulose is expected
256 to occur at the lower temperature range due to its random amorphous structure. The subsequent
257 decomposition of cellulose and lignin follows at higher temperatures as the materials are more
258 ordered and stronger bonded respectively. Biomass has a porous structure providing higher
259 adsorption potential than thermal coal, which is likely to allow large amounts of moisture and
260 carbon dioxide to be absorbed from the atmosphere. These absorbed components are weakly
261 bonded and evolve at the very low temperatures [34]. Cellulose is the main component responsible
262 for the second DTG peak, while lignin is the main component responsible for char formation.
263 However thermal degradation of lignin can start at low temperature at a very slow rate and
264 increases with the increase in temperature [35].

265 Figure 2b shows similar behaviour for coal samples, starting with the small peak at low temperature
266 due to desorption followed by a large single peak due to devolatilisation. The exception for this is
267 with coal B which has produced a clear secondary peak for devolatilisation, meaning coal B goes
268 through extra phase of decomposition. However torrefied grass and charcoal both produced larger
269 initial DTG peaks due to moisture loss followed by two devolatilisation peaks. There is one sharp
270 peak which starts at the temperature of ~ 250 °C and the second peak which is partially
271 superimposed on the late phase of the first peak for torrefied grass. This behaviour is linked to
272 decomposition of cellulose and lignin respectively, while charcoal produces two peaks at much
273 higher temperatures compared to torrefied grass which are from decomposition of lignin and agrees
274 with other researchers' findings on similar materials [15, 35].

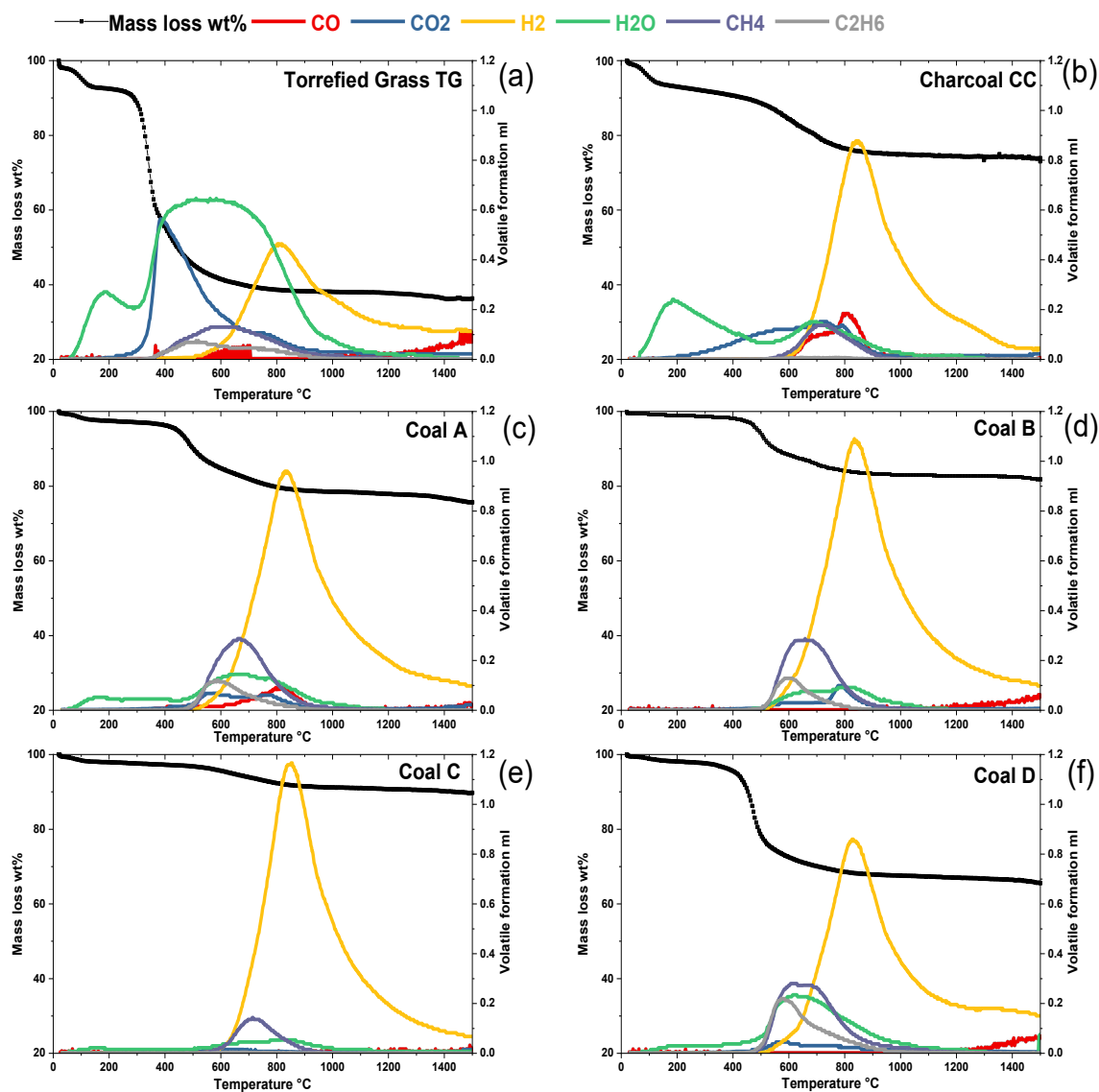
275 3.2. Comparison of devolatilisation behaviours for different carbonaceous materials

276 Various reactions occur simultaneously during devolatilisation upon heating, including break-up of
277 chemical bonds, vaporisation, and condensation or recombination [22]. Using a quadrupole mass
278 spectrometer (QMS) gaseous species evolved during heating process were measured continuously
279 up to the temperature of 1500 °C. Figure 4 shows the mass loss due to devolatilisation measured in
280 TGA tests against the normalized off-gas species measured in the VTF-QMS tests at the heating rate
281 of 10 °C/min for the two biomass and four coal samples.

282 Similar behaviour has been observed for all the samples that gas species detected at low
283 temperature of 100~200 °C were mainly H₂O, as the weight loss at low temperature is associated
284 with the loss of surface moisture. However, at this low temperature range, the weight loss of the
285 biomass samples was significantly higher than that of the coal samples measured, which is
286 confirmed by the amount of these gases detected. Devolatilisation continued with increasing
287 temperature, generating large amount of H₂O and CO₂ gas by biomass samples at temperature of
288 >300 °C while none or very small amount of CO₂ from coal samples was measured **but still significant**
289 **amount of H₂O was produced**. The amount of H₂O and CO₂ produced for torrefied grass during
290 heating was much higher than charcoal, as charcoal has already been pre-treated. However, the
291 amount of gas species generated by charcoal was still significantly higher than that from any of the
292 coal samples tested at similar temperatures, which could be **due to higher oxygen content in the**
293 **charcoal, resulting in the oxidation of carbon and contributing to higher mass loss in charcoal**.

294 The second region of weight loss is associated with the release of organic volatile matter, which
295 started at similar temperatures for all the samples but the gas species generated were different.
296 Both biomass samples started to generate **H₂O and CO₂** at temperature > 300 °C, followed by the
297 release of hydrocarbons at temperature > 400 °C, and H₂ and CO at > 500 °C. The peaks for gases
298 generated in VTF-QMS tests spread over larger temperature range than those observed in TGA tests.
299 This is caused by the gas mixing in the VTF and the time require for evolved gases travelling from the

300 sample location to the detection of mass spectrometer. This travelling distance in the VTF tube gives
301 rise to the comparatively consistent delay for all devolatilisation peaks compared to the TGA results.
302 All the four coal samples tested were found to produce H₂O, CO₂, CH₄, C₂H₆ and H₂ at temperatures >
303 500 °C which corresponds to the region of mass loss in the TGA test results. The H₂O released at
304 temperature >150 °C is associated with the release of inherent moisture which presents in the
305 pore/capillaries of the carbonaceous materials and H₂O produced from decomposition of organic
306 components. It is also known that some H₂O exist as part of the crystal structure of inorganic
307 minerals which can contribute to H₂O formation at higher temperatures [36].

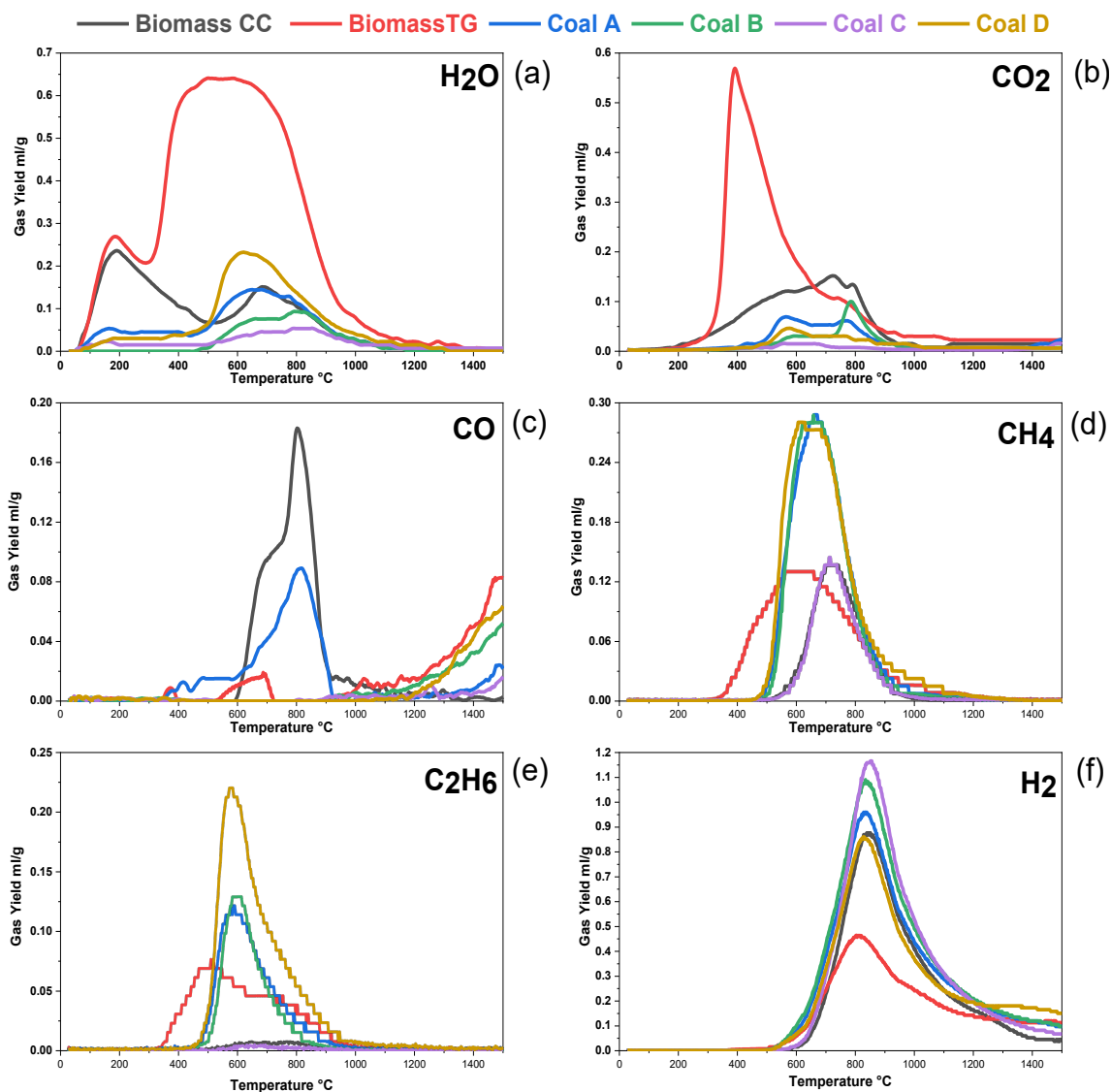


309

310 *Figure 4. VTF-QMS for normalised gas species (CO , CO_2 , H_2 , H_2O , CH_4 , and C_2H_6) evolved against TGA*
 311 *mass loss during heating at the heating rate of $10\text{ }^\circ\text{C}/\text{min}$ under argon atmosphere for (a) Torrefied*
 312 *grass (TG); (b) charcoal (CC), (c) coal A; (d) coal B; (e) coal C; (f) coal D.*

313 The gas products evolved during the heating process are plotted in Figure 5, and some common
 314 phenomena can be observed for the biomass and coal samples. As it can be seen that both charcoal
 315 and torrefied grass samples produced larger amounts of H_2O at low temperature (100 to $200\text{ }^\circ\text{C}$) than
 316 that of all coal samples. Each sample produced a peak for H_2O and CO_2 gas during the heating within
 317 the temperature range of 300 - $800\text{ }^\circ\text{C}$, but the peak for both biomass samples was significantly

318 larger than those for the four coal samples. The sharp H₂O and CO₂ peaks for torrefied grass at the
319 temperature of 300-400 °C links well with the second sharp DTG peak for torrefied grass (shown in
320 Figure 2b) and presents the case that this is due to the release of H₂O and CO₂ from decomposition
321 of hemicellulose and cellulose at that temperature. Charcoal produced a flatter but wide peak of
322 H₂O and CO₂ which may be as a result of the sample already being pre-treated to similar
323 temperatures during the charcoal formation. Previous studies linked the amount and the
324 temperature required for the gas species to be produced to the chemical structure of the biomass
325 component used for the investigation [37]. Hemicellulose is higher in carboxyl content which results
326 in higher CO₂ yield, while cellulose contains carbonyl and carboxyl species which results in CO and
327 CO₂ product yield, and Lignin releases much more H₂ and CH₄ from cracking of aromatic rings and
328 methoxyl [15, 37].



330

331 *Figure 5. An off-gas analysis of (a) H₂O; (b) CO₂; (c) CO; (d) CH₄; (e) C₂H₆; and (f) H₂ evolved during*
 332 *VTF-QMS experiments.*

333 Torrefied grass was the only material which started to produce CH₄ and C₂H₆ at the temperatures
 334 under 400 °C, while all the other samples produced these gases at the temperature > 500 °C. Finally
 335 H₂ and CO formation happened in the higher temperature range which is linked to reactions that
 336 take place at higher activation energy [8, 38]. In addition, the thermal cracking of hydrocarbons is
 337 possible at temperature > 600 °C. The formation of CO and H₂ at high temperature is also linked to
 338 CH₄ reaction with CO₂ to form CO and H₂ [39]. Also hydrocarbons evolved at higher temperatures

339 may react with H₂O to form H₂ and some CO [30, 40] through the reaction schemes presented in
340 equations (4) and (5).



343 4. Kinetic analysis

344 4.1. The Kissinger–Akahira–Sunose method

345 The devolatilisation for carbonaceous materials is a complex process as several reactions occur
346 during thermal decomposition, which includes carbonizing and gas evolution simultaneously during
347 the heating process. For a better understanding of the devolatilisation process, many researchers
348 studied thermal decomposition of carbonaceous materials using TGA technique (which is the most
349 common technique) to measure the weight loss for kinetic analysis. The kinetic parameter obtain are
350 used to understand the complexity of the reaction and in modelling devolatilisation process to
351 predict the mass and energy balances. The devolatilisation mechanism can be described as
352 following: [22]

353 Raw carbonaceous materials \longrightarrow Volatile + Char

354 The devolatilisation conversion and apparent rate of reaction is calculated through equation (6):

$$355 \quad \frac{dx}{dt} = k(T)f(x) \quad (6)$$

356 The temperature dependent reaction rate constant $k(T)$ can be expressed by equation (7):

$$357 \quad k(T) = A e^{\left(\frac{E_x}{RT}\right)} \quad (7)$$

358 By combining equations (6) and (7) the overall reaction conversion rate can be expressed by
359 equation (8):

$$360 \quad \frac{dx}{dt} = A e^{\left(\frac{E_x}{RT}\right)} f(x) \quad (8)$$

361 where x , $\frac{dx}{dt}$, A , E_x , R , T and $f(x)$ denote the devolatilisation conversion degree, reaction conversion
362 rate, pre-exponential factor, activation energy, universal gas constant, temperature and reaction
363 function respectively.

364 The devolatilisation conversion degree(x) is defined by equation (9):

$$365 \quad x = \frac{mi - mt}{mi - mf} \quad (9)$$

366 where mi is the initial weight of the sample, mt is the instant weight of the sample at time t , and
367 mf is the final weight of the sample after the reaction.

368 The experiments are carried out using non-isothermal heating with a constant linear heating rate, β :

$$369 \quad \beta_i = \frac{dT}{dt} \quad (10)$$

370 where i represents the given heating rate being considered.

371 The following equation for reaction conversion rate can be obtained by equations (8) and (10):

$$372 \quad \frac{dx}{dT} = \frac{A}{\beta} e^{\left(\frac{E_x}{RT}\right)} f(x) \quad (11)$$

373 Equation (12) can be obtained by integrating equation (11) to represent the cumulative reaction
374 rate:

$$375 \quad g(x) = \int_0^x (f(x))^{-1} = \frac{A}{\beta} \int_0^T e^{\left(\frac{E_x}{RT}\right)} dT \quad (12)$$

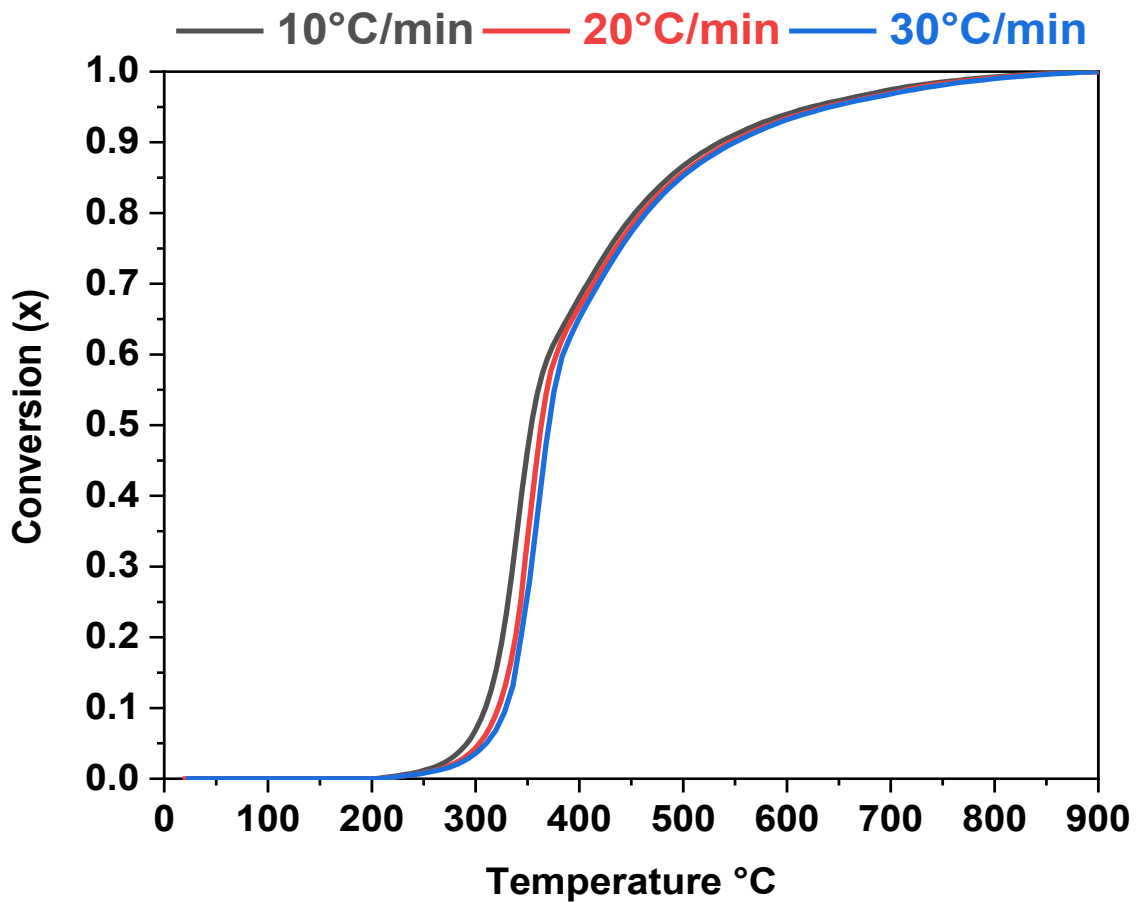
376 where $g(x) = \int_0^x (f(x))^{-1}$ is the integral form of the reaction model [32]. There are several
377 integral methods available which can be used to accurately estimate kinetic parameter. Among them
378 Kissinger–Akahira–Sunose (KAS) model is used by many researchers as a proven model, since the
379 kinetic parameters of a solid state reaction can be obtained without knowing the reaction
380 mechanism and also it is known to have high accuracy in estimating kinetic parameter [10, 31]. The
381 apparent activation energy (E_x) obtained by plotting natural logarithm of heating rate over

382 temperature square at a given value of conversion $\ln\left(\frac{\beta i}{T_{xi}^2}\right)$ versus $\frac{1000}{T_{xi}}$, which is represented by a
383 linear equation (13) for the KAS model for a given value of conversion, x , where the gradient is equal
384 to $-\frac{E_x}{R}$ [41].

$$385 \quad \ln\left(\frac{\beta i}{T_{xi}^2}\right) = \ln\left(\frac{A_x R x}{E_x g x}\right) - \frac{E_x}{RT_{xi}} \quad (13)$$

386 4.2. Kinetic analysis

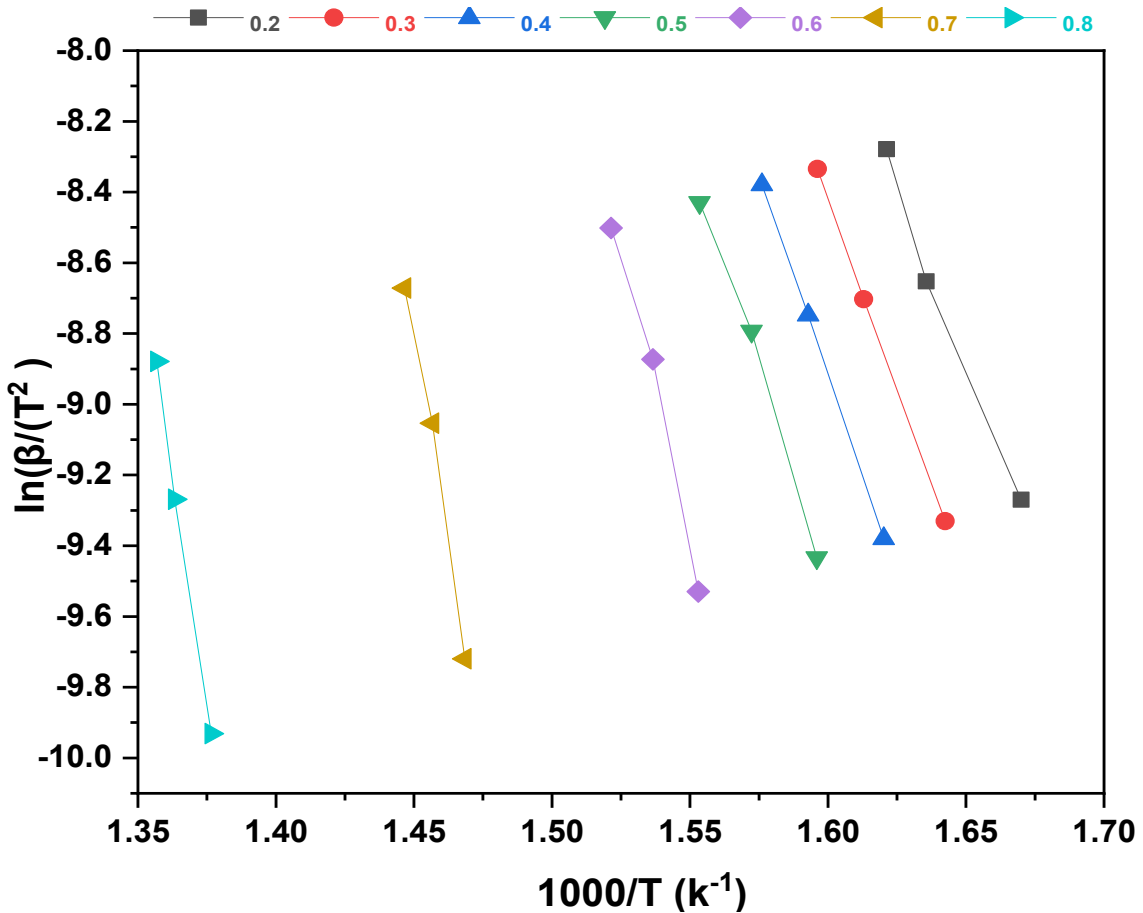
387 The results obtained from the TGA tests at three heating rates (10, 20, and 30 °C/min) are inputted
388 to a calculation according to the KAS method in order to calculate the activation energy (E_a) [10]. As
389 can be seen from off-gas analysis plots in Figure 5, at the temperature of < 200 °C the weight loss is
390 mostly related to surface moisture, with the devolatilisation process related to reducing gases
391 beginning at > 200 °C and then proceeding rapidly to 900 °C. So the devolatilisation conversion
392 degree (x) was calculated according to equation (9) for weight loss in the temperature range of 200-
393 900 °C for all carbonaceous materials tested. Figure 6 shows the devolatilisation conversion
394 degree(x) for torrefied grass (TG) as a function of temperature in TGA tests at the heating rates of
395 10, 20, and 30 °C/min.



396

397 *Figure 6. Extent of conversion curves for the devolatilisation process of torrefied grass (TG) as a*
 398 *function of temperature in TGA tests at different heating rates.*

399 The apparent activation energy from a plot of $\ln\left(\frac{\beta i}{T_{xi}^2}\right)$ versus $\frac{1000}{T_{xi}}$, for a given value of conversion
 400 (x) in the range of 0.2 to 0.8 is shown in Figure 7 for torrefied grass (TG). The average activation
 401 energy is calculated from the gradient equal to $-\frac{E_x}{R}$ and the correlation coefficients. R^2 values
 402 corresponding to the linear lines of best fit were in the range of 0.91 to 1.00 [33] showing good
 403 agreement.



404

405 *Figure 7. KAS plot of torrefied grass (TG) for different values of conversion to calculate the activation*
 406 *energy at different heating rates.*

407 Table 2 contains the calculated variables for all carbonaceous materials tested in this study. It is
 408 seen that the apparent activation energy was not the same for all conversion degrees, which
 409 confirms the occurrence of different reactions at different temperatures during the experiment.

410 Charcoal has quite high and stable E_a values throughout, and the value does not change a lot with
 411 the change in conversion degree probably because of the effects of pre-treatment on this material.

412 Torrefied grass behaved differently, starting with a low E_a value at a low conversion degree and
 413 increasing linearly with an increase of conversion. This may correspond to low E_a values for
 414 decomposition of the remaining hemicellulose and cellulose but higher E_a values for lignin

415 decomposition. Coal A shows a similar behaviour to charcoal with quite stable high E_a values, while
 416 coal B which contains medium volatile matter content has low stable E_a values. Coal C has low E_a

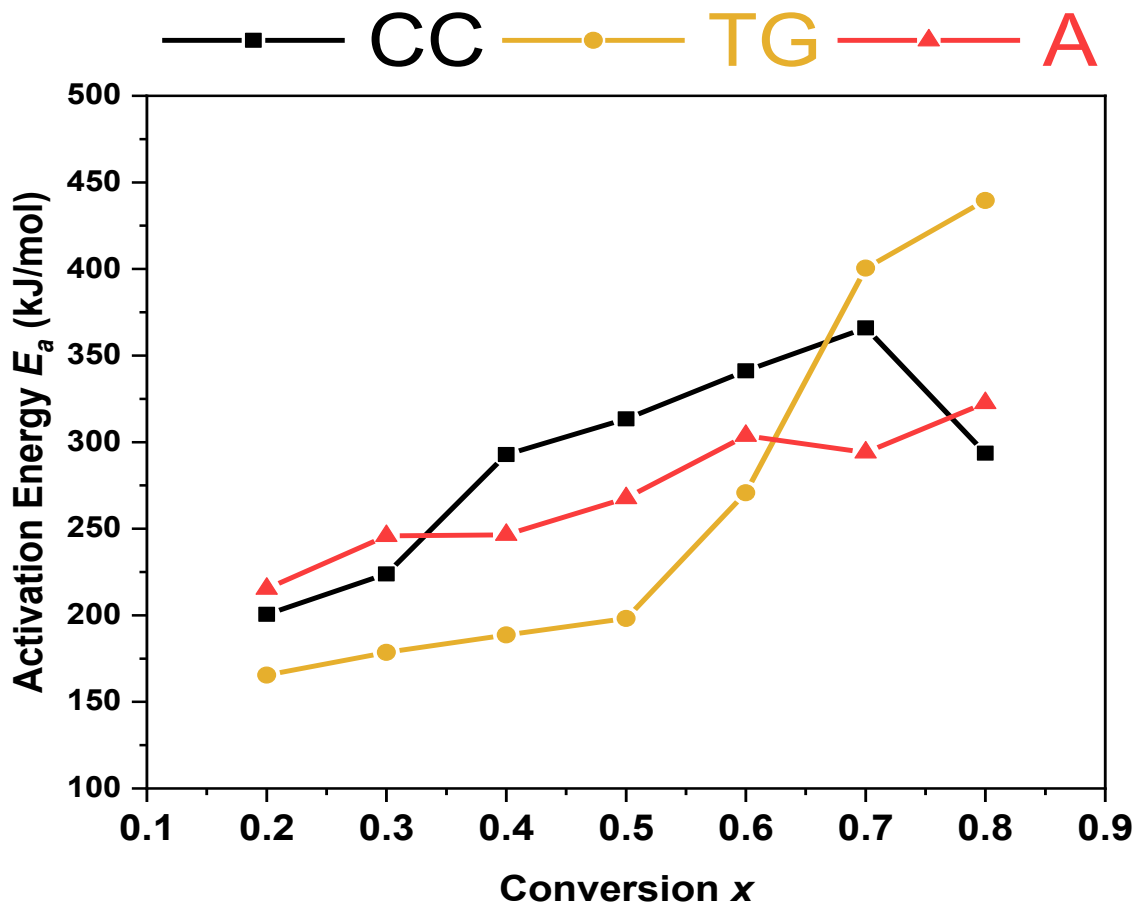
417 value at low conversion degree and increases linearly with an increase in conversion. Coal D starts
 418 with low E_a value at low conversion degree and increases linearly with an increase in conversion
 419 degrees up to 0.6 conversion, and then there is a significant increase in the values at conversion
 420 degrees of 0.7 and 0.8. This behaviour may be influenced by error in the method since the difference
 421 for conversion degrees at different heating rates are not very large, which is seen in Figure 6.

422 *Table 2. Activation energy E_a values in kJ/mol obtained for different carbon sources by using KAS, R^2*
 423 *corresponding to linear fittings*

Conversion (x)	CC		TG		A		B		C		D	
	E_a	R^2	E_a	R^2	E_a	R^2	E_a	R^2	E_a	R^2	E_a	R^2
0.2	201	0.99	165	0.99	215	1.00	183	0.96	77	0.95	192	0.99
0.3	224	1.00	179	1.00	246	1.00	194	0.97	120	0.93	242	0.99
0.4	293	1.00	189	1.00	247	1.00	197	0.97	154	0.93	278	1.00
0.5	313	1.00	198	0.99	268	1.00	193	0.96	185	0.95	311	1.00
0.6	341	1.00	271	0.98	304	1.00	180	0.91	219	0.94	390	0.99
0.7	366	1.00	400	0.99	294	1.00	169	0.92	264	0.95	650	0.98
0.8	294	1.00	440	1.00	323	1.00	173	0.95	335	0.95	1897	95.00
Average E_a	290		263		271		184		194		566	

424 These kinetic models assume the same reactions occurring at a specific conversion degree for
 425 different materials but as it can be observed from Figure 4 that multiple reactions take place at
 426 different temperatures. Therefore it is difficult to make accurate comparison between different
 427 carbon materials. This means the reaction mechanism can change during the devolatilisation
 428 process, therefore E_a is dependent on conversion and the average value of E_a can be estimated as a
 429 function of conversion. Kinetic analysis showed charcoal, torrefied grass and coal A (already injected

430 in Hlsarna trials) have similar average activation energy values (290, 263 and 271 kJ/mol
 431 respectively). Since decomposition of the carbon materials consists of multiple chemical reactions,
 432 the E_a value may change depending on the reactions taking place at specific conversion degree. It
 433 can be noticed in Figure 8 that the value of E_a increases with an increase in conversion.



434

435 *Figure 8. Activation energy E_a as a function of the conversion degree for charcoal (CC), torrefied gas*
 436 *(TG) and Coal A.*

437 The increase in E_a for torrefied grass is notably larger. This is because at low conversion levels very
 438 large amounts of weakly bonded components evolved e.g. H_2O and CO_2 shown in Figure 4 (a),
 439 therefore less energy is required for them to be removed. Charcoal starts with lower E_a at
 440 conversion degrees of 0.2 and 0.3 compared to coal A, but coal A has lower E_a at conversion degree
 441 of 0.4 - 0.7. As can be seen in Figures 4 (b) and (c) charcoal produces larger amount of CO_2 at
 442 temperature where coal A produces more of the other volatiles e.g. CH_4 , C_2H_6 and H_2 at lower

443 temperature which confirms the differences in the E_a values. Based on off-gas analysis and kinetic
444 values charcoal with current properties is the more likely source of biomass which can replace
445 thermal coal in Hlsarna technology, however material handling and pre-treatment may need to be
446 re-considered to optimise its use in the process.

447 **5. Comparison of carbonaceous materials for Hlsarna process**

448 The results of this study indicate that different reactions take place during specific conversion
449 degree for different carbon materials, therefore devolatilisation is affected by the material
450 properties which in turn is linked to volatile mater content. There has been similarities in
451 devolatilisation behaviour (such as devolatilisation temperature), which is essential for smelting
452 reduction vessel in Hlsarna process. Biomass samples produced significantly larger amount of H₂O
453 and CO₂ at low temperatures, however, coal samples produce more CH₄, C₂H₆ and H₂.

454 Despite the pre-treatment of biomass charcoal samples, this study showed that there is still
455 significant weight loss (release of H₂O) at low temperatures because H₂O is absorbed from
456 atmosphere due to their porous structure of the charcoal. Torrefied grass releases a large amount of
457 H₂O and CO₂ at the temperature between 300-400 °C due to its high oxygen potential. These gases
458 and H₂O releasing at lower temperatures can cause temperature drop in the Hlsarna furnace which
459 needs heat compensation and due to high O₂ level much more carbon material may be needed. To
460 avoid these problems and utilise torrefied grass efficiently, a pre-treatment at the temperature of up
461 to 400 °C in inert atmosphere is necessary to reduce the oxygen content and produce bio-chars with
462 similar chemical properties to thermal coal currently used in Hlsarna. To complete this process heat
463 sources from other parts of the steel plant can be utilized to keep the “green” credentials of
464 biomass, the gasses and tars released in the pre-treatment process can be used to generate heat
465 and power for Hlsarna process.

466 Because of the porous structure of biomass carbon sources (e.g. charcoal), material handling needs
467 to be different to avoid H₂O absorption from atmosphere which is evidence in the test results. It may

468 need to consider pre-heating biomass to the temperature of ~ 200 °C before injection to remove all
469 H₂O and other oxide impurities from biomass surface to maintain HIsarna process efficiency. Further
470 studies may be required to investigate the effect of H₂O content in carbonaceous materials on
471 HIsarna process such as materials handling and heat balance.

472 **6. Conclusions**

473 In order to enable the selection of suitable fuel mix in the novel HIsarna ironmaking process, four
474 coals with notable differences in volatile matter content along with two biomass samples sourced
475 from wood and grass origins were investigated in this study. The following conclusions can be
476 obtained.

- 477 • The wt% of reducing gases e.g. H₂, CO, and hydrocarbons, and the temperature required for
478 these gases to evolve was notably different for all the carbonaceous materials tested in this
479 study, but the respective maximum peaks of evolution of these gases corresponded well to the
480 maximum rate of mass loss.
- 481 • The off-gas analysis reveals torrefied grass contains large amount of water and carbon dioxide
482 which will be released at very low temperature, therefore pre-treatment to the temperature of
483 ~ 400 °C is necessary to produce chars with similar properties to coal injected in HIsarna.
- 484 • The change of reactivation energy E_a as a function of conversion degree is determined, which is
485 linked to different reactions at different temperatures.
- 486 • Materials handling needs to be different for biomass (compared to thermal coal) to avoid H₂O
487 absorption.

488 **Acknowledgement**

489 DK would like to thank Tata Steel Nederland Technology BV for providing PhD scholarship (Reference
490 Number: COL1421/GIPS03241) to carry out this research. ZL would like to appreciate the funding
491 from EPSRC under the grant number EP/N011368/1. The authors appreciate Tata Steel HIsarna team
492 for fruitful discussions and providing samples. DK also would like to thank Dr. Ian Moore at Material

493 Processing Institute for providing coal C and coal D samples, and Tata Steel IJmuiden would like to
494 acknowledge OrangeGreen BV for providing the torrefied grass sample.

495 **References:**

- 496 [1] Hasanbeigi, A., Arens, M. & Price, L. Alternative emerging ironmaking technologies for energy-
497 efficiency and carbon dioxide emissions reduction : A technical review. *Renewable and*
498 *Sustainable Energy Reviews* 33, 645-658 (2014).
- 499 [2] Suopajarvi, H. et al. Use of biomass in integrated steelmaking – Status quo, future needs and
500 comparison to other low-CO₂ steel production technologies. *Appl. Energy* 213, 384–407
501 (2018).
- 502 [3] Abdul Quader, M., Ahmed, S., Dawal, S. Z. & Nukman, Y. Present needs, recent progress and
503 future trends of energy-efficient Ultra-Low Carbon Dioxide (CO₂) Steelmaking (ULCOS)
504 program. *Renew. Sustain. Energy Rev.* 55, 537–549 (2016).
- 505 [4] Meijer, K., Zeilstra, C., Teerhuis, C., Ouwehand, M. & Van Der Stel, J. Developments in
506 alternative ironmaking. *Trans. Indian Inst. Met.* (2013). doi:10.1007/s12666-013-0309-z
- 507 [5] Meijer, K., Guenther, C. & Dry, R. J. Hlsarna Pilot Plant Project. *InSteelCon* 1–5 (2011).
- 508 [6] TEASDALE, S. and HAYES, P., 2005. Observations of the Reduction of FeO from Slag by
509 Graphite, Coke and Coal Char. *ISIJ International*, 45(5), pp.634-641.
- 510 [7] Boggelen, J., Meijer, K., Zeilstra, C., Hage, H. and Broersen, P. (2019). Hlsarna - Demonstrating
511 low CO₂ ironmaking at pilot scale.
- 512 [8] Yu, J., Lucas, J. and Wall, T., 2007. Formation of the structure of chars during devolatilisation
513 of pulverized coal and its thermoproperties: A review. *Progress in Energy and Combustion*
514 *Science*, 33(2), pp.135-170.
- 515 [9] Chen, L., Zeng, C., Guo, X., Mao, Y., Zhang, Y., Zhang, X., Li, W., Long, Y., Zhu, H., Eiteneer, B.
516 and Zamansky, V. (2010). Gas evolution kinetics of two coal samples during rapid pyrolysis.
517 *Fuel Processing Technology*, 91(8), pp.848-852.

- 518 [10] Slopiecka, K., Bartocci, P. and Fantozzi, F. (2012). Thermogravimetric analysis and kinetic study
519 of poplar wood pyrolysis. *Applied Energy*, 97, pp.491-497.
- 520 [11] Gašparovič, L., Koreňová, Z. and Jelemenský, Ľ. (2010). Kinetic study of wood chips
521 decomposition by TGA. *Chemical Papers*, 64(2).
- 522 [12] van Heek, K. and Hodek, W. (1994). Structure and pyrolysis behaviour of different coals and
523 relevant model substances. *Fuel*, 73(6), pp.886-896.
- 524 [13] Anca-Couce, A. and Obernberger, I. (2016). Application of a detailed biomass pyrolysis kinetic
525 scheme to hardwood and softwood torrefaction. *Fuel*, 167, pp.158-167.
- 526 [14] Dwivedi, K., Chatterjee, P., Karmakar, M. and Pramanick, A. (2019). Pyrolysis characteristics
527 and kinetics of Indian low rank coal using thermogravimetric analysis. *International Journal of*
528 *Coal Science & Technology*, 6(1), pp.102-112.
- 529 [15] Ren, S.; Lei, H.; Wang, L.; Bu, Q.; Chen, S.; Wu, J. Thermal behaviour and kinetic study for
530 woody biomass torrefaction and torrefied biomass pyrolysis by TGA. *Biosyst. Eng.* 2013, 116,
531 420–426, doi:10.1016/j.biosystemseng.2013.10.003.
- 532 [16] Liu, J., Jiang, X., Shen, J. and Zhang, H. (2014). Pyrolysis of superfine pulverized coal. Part 1.
533 Mechanisms of methane formation. *Energy Conversion and Management*, 87, pp.1027-1038.
- 534 [17] Ferdous, D., Dalai, A., Bej, S., Thring, R. and Bakhshi, N. (2001). Production of H₂ and medium
535 Btu gas via pyrolysis of lignins in a fixed-bed reactor. *Fuel Processing Technology*, 70(1), pp.9-
536 26.
- 537 [18] Yan, X., Che, D. and Xu, T. (2005). Effect of rank, temperatures and inherent minerals on
538 nitrogen emissions during coal pyrolysis in a fixed bed reactor. *Fuel Processing Technology*,
539 86(7), pp.739-756.
- 540 [19] Heidari, A., Stahl, R., Younesi, H., Rashidi, A., Troeger, N. and Ghoreyshi, A. (2014). Effect of
541 process conditions on product yield and composition of fast pyrolysis of *Eucalyptus grandis* in
542 fluidized bed reactor. *Journal of Industrial and Engineering Chemistry*, 20(4), pp.2594-2602.

- 543 [20] Zhang, X., Dong, L., Zhang, J., Tian, Y. and Xu, G. (2011). Coal pyrolysis in a fluidized bed
544 reactor simulating the process conditions of coal topping in CFB boiler. *Journal of Analytical
545 and Applied Pyrolysis*, 91(1), pp.241-250.
- 546 [21] Biagini, E., Barontini, F. and Tognotti, L. (2006). Devolatilisation of Biomass Fuels and Biomass
547 Components Studied by TG/FTIR Technique. *Industrial & Engineering Chemistry Research*,
548 45(13), pp.4486-4493.
- 549 [22] Xu, R., Zhang, J., Wang, G., Zuo, H., Liu, Z., Jiao, K., Liu, Y. and Li, K. (2016). Devolatilisation
550 Characteristics and Kinetic Analysis of Lump Coal from China COREX3000 Under High
551 Temperature. *Metallurgical and Materials Transactions B*, 47(4), pp.2535-2548.
- 552 [23] Chen, D., Liu, D., Zhang, H., Chen, Y. and Li, Q. (2015). Bamboo pyrolysis using TG–FTIR and a
553 lab-scale reactor: Analysis of pyrolysis behavior, product properties, and carbon and energy
554 yields. *Fuel*, 148, pp.79-86.
- 555 [24] Bassilakis, R., Carangelo, R. and Wójtowicz, M. (2001). TG-FTIR analysis of biomass pyrolysis.
556 *Fuel*, 80(12), pp.1765-1786.
- 557 [25] Zhang, X., Dong, L., Zhang, J., Tian, Y. and Xu, G. (2011). Coal pyrolysis in a fluidized bed
558 reactor simulating the process conditions of coal topping in CFB boiler. *Journal of Analytical
559 and Applied Pyrolysis*, 91(1), pp.241-250.
- 560 [26] Han, F., Meng, A., Li, Q. and Zhang, Y. (2016). Thermal decomposition and evolved gas analysis
561 (TG-MS) of lignite coals from Southwest China. *Journal of the Energy Institute*, 89(1), pp.94-
562 100.
- 563 [27] Li, x., Matuschek, G., Herrera, M., Wang, H. and Kettrup, A. (2002). Investigation of pyrolysis of
564 Chinese coals using thermal analysis/mass spectrometry. *Thermal Analysis and Calorimetry*,
565 71, pp.601–612.
- 566 [28] Arenillas, A., Rubiera, F. and Pis, J. (1999). Simultaneous thermogravimetric–mass
567 spectrometric study on the pyrolysis behaviour of different rank coals. *Journal of Analytical
568 and Applied Pyrolysis*, 50(1), pp.31-46.

- 569 [29] Wannapeera, J., Fungtammasan, B. and Worasuwanarak, N. (2011). Effects of temperature
570 and holding time during torrefaction on the pyrolysis behaviors of woody biomass. *Journal of*
571 *Analytical and Applied Pyrolysis*, 92(1), pp.99-105.
- 572 [30] Jayaraman, K., Kok, M. and Gokalp, I. (2017). Thermogravimetric and mass spectrometric (TG-
573 MS) analysis and kinetics of coal-biomass blends. *Renewable Energy*, 101, pp.293-300.
- 574 [31] El-Tawil, A., Ökvist, L., M. Ahmed, H. and Björkman, B. (2019). Devolatilisation Kinetics of
575 Different Types of Bio-Coals Using Thermogravimetric Analysis. *Metals*, 9(2), p.168.
- 576 [32] Qiao, Y., Chen, S., Liu, Y., Sun, H., Jia, S., Shi, J., Pedersen, C., Wang, Y. and Hou, X. (2015).
577 Pyrolysis of chitin biomass: TG–MS analysis and solid char residue characterization.
578 *Carbohydrate Polymers*, 133, pp.163-170.
- 579 [33] Borah, R., Ghosh, P. and Rao, P. (2011). A review on devolatilisation of coal in fluidized bed.
580 *International Journal of Energy Research*, 35(11), pp.929-963.
- 581 [34] Yang, H., Yan, R., Chen, H., Zheng, C., Lee, D. and Liang, D. (2006). In-Depth Investigation of
582 Biomass Pyrolysis Based on Three Major Components: Hemicellulose, Cellulose and Lignin.
583 *Energy & Fuels*, 20(1), pp.388-393.
- 584 [35] Yang, H., Yan, R., Chen, H., Lee, D. and Zheng, C. (2007). Characteristics of hemicellulose,
585 cellulose and lignin pyrolysis. *Fuel*, 86(12-13), pp.1781-1788.
- 586 [36] Zhu, Q., 2014. *Coal Sampling And Analsis Standards*. [online] Usea.org. Available at:
587 <[https://usea.org/sites/default/files/042014_Coal%20sampling%20and%20analysis%20standar](https://usea.org/sites/default/files/042014_Coal%20sampling%20and%20analysis%20standards_ccc235.pdf)
588 [ds_ccc235.pdf](https://usea.org/sites/default/files/042014_Coal%20sampling%20and%20analysis%20standards_ccc235.pdf)> [Accessed 25 June 2020].
- 589 [37] Werner, K., Pommer, L. and Broström, M. (2014). Thermal decomposition of hemicelluloses.
590 *Journal of Analytical and Applied Pyrolysis*, 110, pp.130-13.
- 591 [38] Yang, H., Yan, R., Chen, H., Lee, D., Liang, D. and Zheng, C. (2006). Mechanism of Palm Oil
592 Waste Pyrolysis in a Packed Bed. *Energy & Fuels*, 20(3), pp.1321-1328.
- 593 [39] Halmann, M., 2018. *Chemical Fixation Of Carbon Dioxidemethods For Recycling CO2 Into*
594 *Useful Products*. Boca Raton: Chapman and Hall/CRC.

- 595 [40] Basile, A., Centi, G., De Falco, M. and Iaquaniello, G., 2019. Catalysis, Green Chemistry And
596 Sustainable Energy. 1st ed. San Diego: Elsevier, pp.284-288.
- 597 [41] Kissinger, H. (1956). Variation of peak temperature with heating rate in differential thermal
598 analysis. Journal of Research of the National Bureau of Standards, 57(4), p.217

*Declaration of Interest Statement

Declaration of interests

The authors declare that they have no known competing financial interests or personal relationships that could have appeared to influence the work reported in this paper.

The authors declare the following financial interests/personal relationships which may be considered as potential competing interests:

CRedit author statement:

Darbaz Khasraw: Conceptualization, Methodology, Validation, Formal analysis, Investigation, Resources, Writing - Original Draft, Writing - Review & Editing, Visualization, Supervision, Project administration **Stephen Spooner:** Conceptualization, Writing - Review & Editing, Supervision, **Hans Hage:** Conceptualization, Resources **Koen Meijer:** Conceptualization, Resources, Writing - Review & Editing, Supervision **Zushu Li:** Conceptualization, Validation, Writing - Review & Editing, Supervision, Project administration, Funding acquisition.

Author names:

Darbaz Khasraw ^a, Stephen Spooner ^a, Hans Hage ^b, Koen Meijer ^b, Zushu Li ^a

Affiliations:

^a WMG, Advanced Manufacturing & Materials Centre, University of Warwick, Coventry, CV4 7AL, United Kingdom

Darbaz Khasraw: d.khasraw@warwick.ac.uk

Stephen Spooner: s.spooner@warwick.ac.uk

Zushu Li: z.li.19@warwick.ac.uk

^b Tata Steel IJmuiden, PO Box 10000,1970CA IJmuiden, The Netherlands

Hans Hage: hans.hage@tatasteelurope.com

Koen Meijer: koen.meijer@tatasteelurope.com

Corresponding author:

Corresponding author. Tel.: +44 (0)24 7652 4706

E-mail address: d.khasraw@warwick.ac.uk (D. Khasraw)

Postal address: WMG, University of Warwick, Coventry CV4 7AL, UK